Preprint
UCRL-JC-139232-PT-1-REV-1

Uranyl-Fluoride (^{233}U) Solutions in Spherical Stainless Steel Vessels with Reflectors of Be, Ch_2 and Be-Ch_2 Composites

D. Heinrichs

This article was submitted to
International Criticality Safety Benchmark Evaluation Project
Working Group Meeting, Jackson Hole, WY, June 11-15, 2001

U.S. Department of Energy

Lawrence
Livermore
National
Laboratory

April 24, 2001

ACKNOWLEDGEMENTS

The author is pleased to acknowledge that this evaluation is primarily based on the unpublished work of H. Robert Ralston who was the principal experimenter for the *Falstaff* series of experiments. The author has also relied heavily on unpublished work by J. Carothers, F. A. Kloverstrom, O. C. Kolar and A. J. Reyenga.

This work was performed under the auspices of the U.S. Department of Energy by the University of California, Lawrence Livermore National Laboratory under Contract No. W-7405-Eng-48.

U233-SOL-INTER-001

URANYL-FLUORIDE (^{233}U) SOLUTIONS IN SPHERICAL STAINLESS STEEL VESSELS WITH REFLECTORS OF Be, CH_2 AND Be-CH_2 COMPOSITES

IDENTIFICATION NUMBER: U233-SOL-INTER-001

KEY WORDS: acceptable, beryllium, beryllium-reflected, critical experiments, Falstaff, homogeneous solution, polyethylene, polyethylene-reflected, solution, sphere, spherical assembly, ^{233}U, uranyl-fluoride, water-moderated

1.0 DETAILED DESCRIPTION

1.1 Overview of Experiments

A series of criticality studies were performed at the Lawrence Livermore National Laboratory in the late 1950's using aqueous solutions of ^{233}U in the form of UO_2F_2 stabilized with 0.3% by weight of HF. The ^{233}U concentration in these experiments ranged from 0.13 to 0.87 kg/l. Eight type 347 stainless steel spheres ranging in inner radius from 7.87 to 12.45 cm were available for use as containers for the solutions.

The scope of this evaluation is limited to the experiments involving the three highest concentrations of uranyl-fluoride solution. The seven smallest spheres were used in these experiments with 0.87, 0.75 and 0.57 kg/l ^{233}U solutions. Reflectors of beryllium, polyethylene and beryllium-polyethylene composites were used. Thirty-three configurations are evaluated and accepted as criticality-safety benchmark models. Calculated fission spectra are provided in Appendix B which show that twenty-three of these configurations have intermediate fission spectra, six have mixed fission spectra and three have thermal fission spectra.

These experiments were assigned the program name *Falstaff* and are published here for the first time. These experiments are believed to be unique in that they provide critical data for uranyl-fluoride aqueous solutions with concentrations higher than that achieved at any other laboratory.

1.2 Description of the Experimental Configuration

Photographs of the experimental assembly and equipment are provided as Figures 1 - 3. A view of the vertical lift machine with an experimental assembly is provided in Figure 1. One stainless steel hollow spherical vessel is located in the central cavity of the lower set of nested hemispherical reflector shells. The lower assembly is positioned on the hydraulic ram. The tube used to transfer solution into the experimental vessel is shown in the lower part of this figure. The upper-reflector hemispherical shells were suspended by a support rod from the upper fixed support structure of the vertical lift machine. The lower subassembly was remotely raised by the hydraulic ram to seat within the upper reflector hemispherical shells to complete the experimental assembly configuration. Positive-stop spacers were

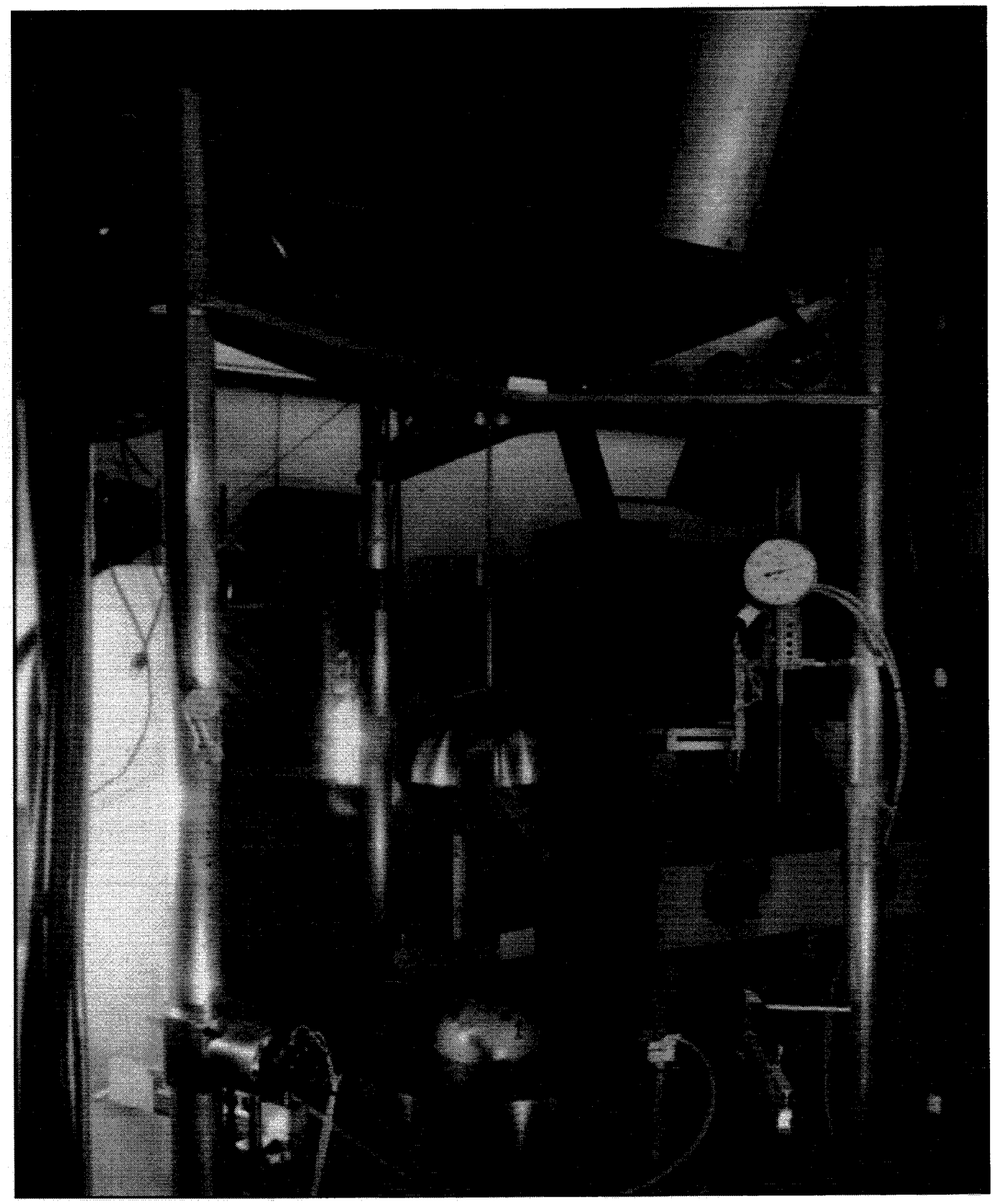

Figure 1. View of the Vertical Lift Machine with an Assembly.

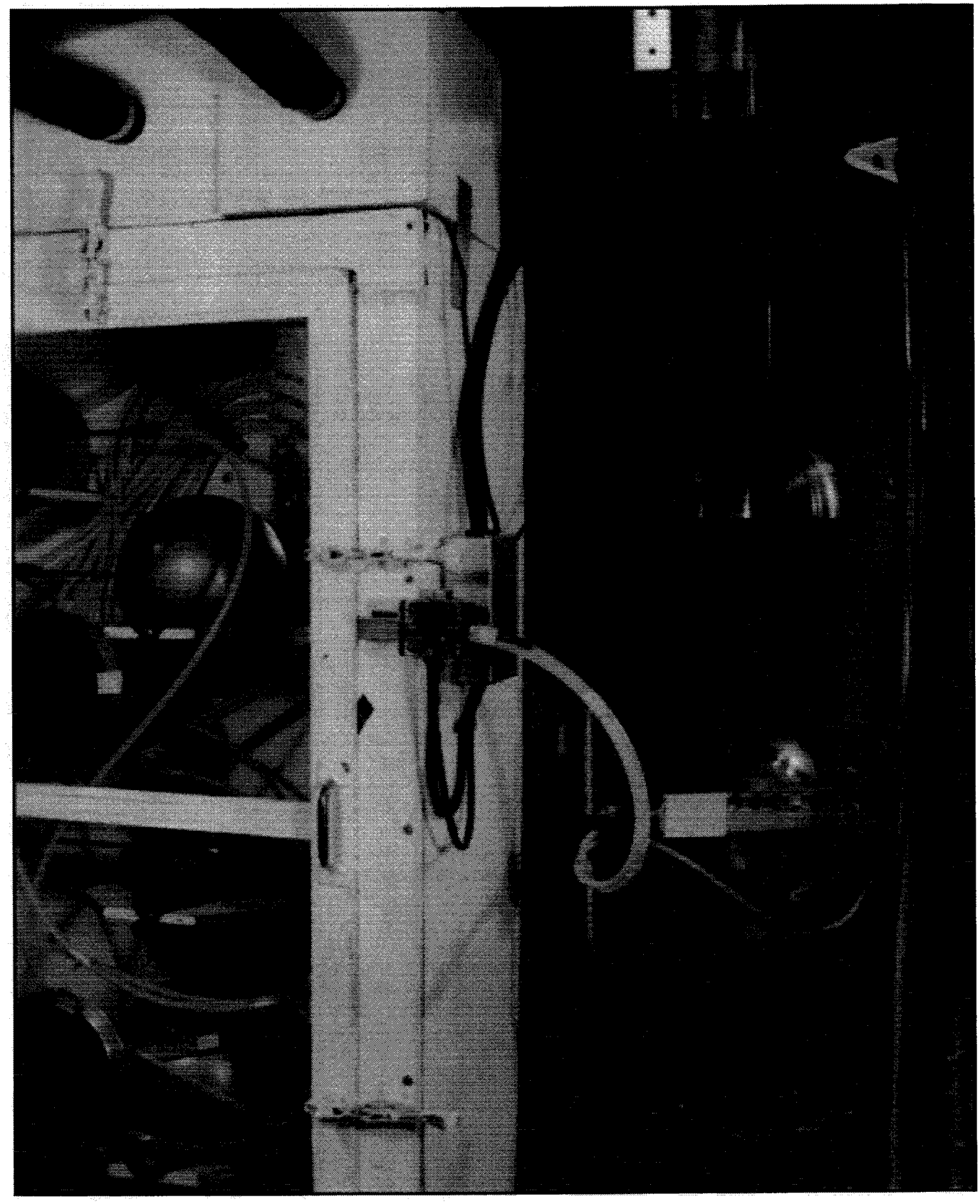

Figure 2. View Showing the Connection to the Solution Handling System.

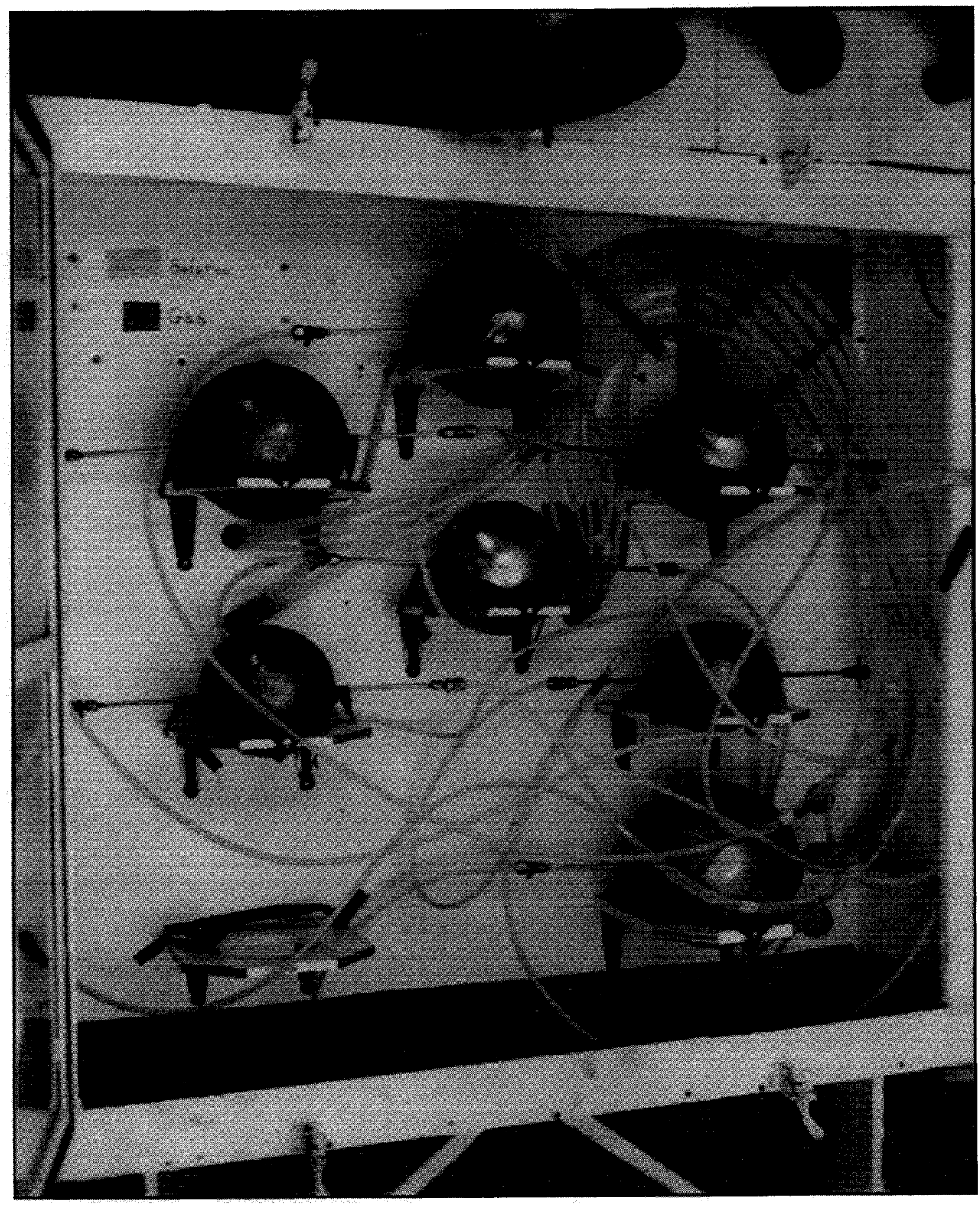

Figure 3. Storage Box for the Stainless Steel Spherical Solution Vessels.

sometimes used to perform an assembly in steps at known separation distances between top and bottom reflector halves.

A portion of the solution handling system is shown in Figure 2. Figure 3 shows seven of the eight available spherical vessels in their storage box. A total of eight different spherical shell sizes, each constructed of type 347 stainless steel (SS-347), with an average wall thickness of about 0.019 inch, were used in the *Falstaff* experiments. The nominal outer diameter, measured capacities and inner diameters calculated from the measured capacities of these shells are given in Table 1.

Table 1. Dimensions and Capacities of the Spherical Vessels.

Sphere No.	Nominal Outer Diameter (inches)	Measured Capacity (grams of water)	Calculated Inner Diameter (inches)
1	6.3	2043.82	6.198
2	6.8	2586.31	6.705
3	7.2	3061.72	7.093
4	7.7	3779.80	7.609
5	8.1	4396.27	8.002
6	8.6	5275.53	8.503
7	9.1	6230.69	8.988
8	9.9	8095.95	9.808

The calculated inner diameters were based on the measured capacities by assuming one gram of water is equivalent to one milliliter of volume as stated by the experimenter (see Section 2.2.1).

1.2.1 Description of the Experimental Procedure - The first series of experiments performed with each concentration of uranyl-fluoride solution were safety tests to determine the multiplication of the unreflected spheres. These experiments commenced with the smallest spheres which were certain to be subcritical. A plot of the measured reciprocal multiplication (1/M) versus sphere radius was used to estimate the unreflected critical radius for each solution by extrapolation. In the case of the three highest concentration solutions, these extrapolations result in large experimental uncertainties; and consequently, these experiments are not evaluated but are included in Section 1.4.

Following the unreflected experiments, measurements using the thinnest reflectors with the smallest sphere were performed. Subsequent reflector shells were then added in accordance with the shape of the reciprocal multiplication curve versus reflector thickness. The available nesting reflector shells were designed so that steps of 0.5 cm in reflector thickness were available in the expected critical region. When the multiplication was expected to exceed fifty, closure was carried out in steps of decreasing separation between top and bottom reflector halves using positive-stops. Multiplications in excess of one hundred were not exceeded. Criticality was predicted by extrapolation from the measured reciprocal multiplication measurements. This experimental procedure was then repeated for the next largest sphere and so on.

1.2.2 Summary of the Experimental Results - A summary of the critical parameters for the three highest concentration aqueous uranyl-fluoride solution experiments is given Table 2. Note that uncertainties in the critical reflector thickness were recorded only for the beryllium reflected experiments. Details of the ^{233}U solution are provided in Section 1.3.

Table 2. Critical Parameters for Spherical Systems of ^{233}U in Aqueous Solution.

Solution No.	Sphere No.	^{233}U Mass (kg)	Critical Reflector Thickness (cm)		
			Be	CH_2	Be + CH_2
1	1	1.77	8.00 ± 1.5%	---	---
	2	2.25	5.82 ± 2.3%	---	---
	3	2.66	4.67 ± 1.0%	--- [(a)]	1.14 + 4.11
	4	3.28	3.50 ± 3.0%	---	0.51 + 3.31
	5	3.82	2.69 ± 2.0%	3.05	1.27 + 1.47
	6	4.58	1.83 ± 2.0%	---	0.64 + 1.35
2	1	1.54	8.00 ± 2.0%	---	---
	2	1.94	5.94 ± 1.0%	---	1.65 + 5.18
	3	2.30	4.70 ± 2.0%	11.68	1.14 + 4.06
	4	2.84	3.43 ± 1.0%	---	---
	5	3.30	2.62 ± 4.0%	3.07	---
	6	3.96	1.78 ± 2.0%	---	---
	7	4.68	1.18 ± 3.0%	1.52	---
3	1	1.16	8.69 ± 1.5%	---	---
	2	1.47	6.20 ± 2.0%	---	---
	3	1.74	5.03 ± 1.0%	--- [(b)]	1.14 + 4.34
	4	2.15	3.61 ± 1.5%	---	---
	5	2.50	2.72 ± 5.0%	3.10	---
	6	3.00	2.08 ± 4.0%	---	---
	7	3.55	1.19 ± 4.0%	1.60	---

[(a)] Critical thickness exceeds 8.38 cm and an infinite thickness of CH_2 is probably subcritical. [(b)] An infinite thickness of CH_2 is sub-critical.

Note that with composite beryllium-polyethylene reflectors, the beryllium is inside the polyethylene.

No temperature measurements were performed; however, the experimenters assumed constant ambient temperatures of about 20°C (70°F) for the entire series of experiments.

1.3 Description of Material Data

Seven concentrations of aqueous uranyl-fluoride solutions were used in the *Falstaff* series of experiments, starting with the most concentrated and diluting as the series progressed. The properties of the three highest concentration solutions are provided in Table 3.

Table 3. Properties of Aqueous Uranyl-Fluoride Solutions.

Solution Density	Fissile Concentration	HF Content
1.9712 g/ml	0.87 g^{233}U/ml	0.3 wt-%
1.8386 g/ml	0.75 g^{233}U/ml	0.3 wt-%
1.6357 g/ml	0.60 g^{233}U/ml	0.3 wt-%

The isotopic composition of the elemental uranium is given in Table 4. Note that these isotopic values represent the average of several determinations and therefore sum to 100.0073% instead of exactly 100%. Unfortunately, no information on uncertainties, thorium content, or other impurities are available.

Table 4. Uranium Isotopics.

Isotope	Percent (by weight)
^{232}U	0.0020
^{233}U	98.562
^{234}U	1.0755
^{235}U	0.0398
^{238}U	0.328

The spherical vessels were made of about 0.019-inch-thick type 347 stainless steel with the elemental composition listed in Table 5. The density of type 347 stainless steel is 8.0 g/cm^3.

Table 5. Type 347 Stainless Steel Material Specifications.

Element	Percent by weight
Cr	17 – 19
Ni	9 – 13
Mn	≤2
Nb + Ta	0.3 – 1.0
Si	≤0.75
C	≤0.08
P	≤0.045
S	≤0.030
Fe	Balance

All reflectors were an assemblage of close-fitting nesting spherical shells with the innermost shells fitting closely around the solution container. Tolerance gaps at the spherical interfaces introduced small voids into the reflectors. All reflectors had 0.25-inch-diameter support holes (diametrically opposed at the pole) in both the top and bottom. These holes extended from the outer surface of the reflector to the surface of the solution container. There were two additional 0.25-inch holes (diametrically opposed at the waist) to accommodate the fill tube for introduction of the ^{233}U solution.

The bottom hemispherical shell of every beryllium reflector had a 2-inch-diameter hole extending all the way through it. These holes were plugged by the removed section, leaving only a 0.0625-inch gap around the plug. There was also an unplugged 0.5-inch diameter hole extending through each beryllium reflector to accommodate placement of a neutron source. However, no external neutron sources were used in these experiments.

The various gaps and holes in the reflectors result in an average bulk reflector density which is slightly lower than the nominal value. The beryllium reflector had an effective average bulk density of 1.82 +0.02/-0.03 g/cm^3 as listed in Table 6. This was determined experimentally by weighing and measuring various sets of nested shells. The average bulk density of the polyethylene reflectors was not measured but was assumed by the experimenter to be about 0.92 g/cm^3. Hence, a reasonable estimate of the range is 0.92 $\pm$ 0.010 g/cm^3 as entered in Table 6.

Table 6. Reflector Average Bulk Densities.

Reflector Material	Average Bulk Density (g/cm^3)		
	Minimum	Nominal	Maximum
Beryllium	1.79	1.82	1.84
Polyethylene	0.91	0.92	0.93

Typical commercially pure beryllium metal contains at most 2 percent by weight of beryllium oxide with other minor impurities as listed in Table 7. Polyethylene is CH_2.

Table 7. Typical Specification for Beryllium Metal.

Impurity	Maximum Weight Percentage
BeO	2.00
N	0.06
C	0.15
Fe	0.20
Al	0.16
Si	0.12
Mg	0.08
Mn	0.05
Sum of Cr, Cu, Ni, Ti	0.20
Any other	0.05

1.4 Supplemental Experimental Measurements

The detailed results of the safety tests with the unreflected spheres described in Section 1.2.1 have yet to be found. However, the experimenter's estimates of the critical radius extrapolated from these experiments are reported below.

Table 8. Extrapolated Critical Radii[a].

Solution No.	Radius (cm)
1	11.9 ± 31%
2	12.7 ± 25%
3	12.72 ± 7%

[a]Bare 0.019" SS-347 Spheres.

2.0 EVALUATION OF EXPERIMENTAL DATA

This section reports the results of sensitivity studies performed to determine the effect on k_{eff} of various uncertainties in the reported experimental data. A summary of the benchmark or nominal values of the significant parameters and their uncertainty range is provided in Table 9. The details of the calculated uncertainties in k_{eff}, or Δk_{eff}, for each parameter applicable to each experiment, are provided in the sections. These k_{eff} calculations used the SAN code, which is a LLNL[a]-modified (short) version of ANISN, with a 92-energy-group cross-section library. The calculations were run in the $S_{12}P_3$ approximation. An estimate of the total minimum, maximum, and standard uncertainty for each experiment is provided in Section 2.5.

Table 9. Uncertainties in the *Falstaff* Experiments.

Material	Parameter	Benchmark-Model or Nominal Value	Uncertainty Range
Solution No. 1	^{233}U concentration	0.866 g/ml	± 0.003 g/ml
	Solution density	1.9712 g/ml	± 0.0005 g/ml
Solution No. 2	^{233}U concentration	0.749 g/ml	± 0.003 g/ml
	Solution density	1.8386 g/ml	± 0.0005 g/ml
Solution No. 3	^{233}U concentration	0.5672 g/ml	± 0.0026 g/ml
	Solution density	1.6357 g/ml	± 0.0005 g/ml
All Solutions	HF content (all solutions)	0.3 wt-%	± 0.05 wt-%
	^{233}U enrichment	98.562 wt-%	± 0.005 wt-%
SS-347 Vessel	Capacity	See Table 1	+0.5 vol-%
	Chemical composition	See Table 5	See Section 2.2
	Thickness	0.019 inch	± 0.0005 inch
	Density	8.0 g/cm^3	± 0.05 g/cm^3
Reflector	Critical thickness	See Table 2	±1% to 3%
	Bulk density	See Table 6	See Table 6
	Impurities in beryllium	Pure	See Table 7
Exterior	Room return	None	See Section 2.3

The benchmark-model values are the same as the nominal experimental values described in Section 1 with one exception. The fissile ^{233}U concentrations are taken as 0.866 ± 0.003 g/ml, 0.749 ± 0.003 and 0.5672 ± 0.003 g/ml as shown above and discussed in Section 2.1.1.

The total uncertainty is principally due to the uncertainties in the critical reflector thickness, reflector density, beryllium impurities, fissile concentration and vessel capacity. The other sources of uncertainty are not significant.

[a] Lawrence Livermore National Laboratory

2.1 Solution Uncertainties

2.1.1 Uncertainty in Fissile Concentrations - The fissile ^{233}U concentration of the solutions are reported as 0.87, 0.75 and 0.60 $g^{233}U/ml$; however, the values 0.866 ± 0.003, 0.749 ± 0.003 and 0.5672 ± 0.0026 $g^{233}U/ml$ may be obtained by dividing each reported critical mass given in Table 2 by the measured vessel capacity listed in Table 1. The capacities are given as grams of water and the water density is assumed to be either 0.995 or 1.000 g/cm^3 as discussed in Section 2.2.1. This procedure results in an improved estimate of the actual solution densities with the specified mean and standard deviation consistent with the reported value.

A sensitivity study was performed to consider changes of 0.866 ± 0.003, 0.749 ± 0.003 and 0.5672 ± 0.0026 $g^{233}U/ml$ in the fissile concentration with the total solution density unchanged. Consequently, an increase in fissile content results in a decrease in the moderator content; and, vice versa. The results of these sensitivity calculations are reported together with the benchmark-model results in Table 10.

Table 10. Effect on k_{eff} due to Uncertainty in the Fissile Concentration.

Sphere No.	Reflector	^{233}U Concentration			Change (Δk_{eff})
		Maximum	Nominal	Minimum	
Solution No. 1		*0.869 g/ml*	*0.866 g/ml*	*0.863 g/ml*	—
1	Be	0.9933	0.9954	0.9974	+0.0020 -0.0021
2	Be	0.9912	0.9934	0.9957	+0.0023 -0.0022
3	Be	0.9925	0.9949	0.9973	+0.0024 -0.0024
3	Be + CH_2	1.0002	1.0024	1.0046	+0.0022 -0.0022
4	Be	0.9958	0.9984	1.0010	+0.0026 -0.0026
4	Be + CH_2	0.9934	0.9958	0.9982	+0.0024 -0.0024
5	Be	0.9929	0.9956	0.9984	+0.0028 -0.0027
5	CH_2	0.9881	0.9906	0.9931	+0.0025 -0.0025
5	Be + CH_2	0.9898	0.9925	0.9952	+0.0027 -0.0027
6	Be	0.9893	0.9922	0.9952	+0.0030 -0.0029
6	Be + CH_2	0.9899	0.9927	0.9956	+0.0029 -0.0028
Solution No. 2		*0.752 g/ml*	*0.749 g/ml*	*0.746 g/ml*	—
1	Be	0.9888	0.9908	0.9928	+0.0020 -0.0020
2	Be	0.9920	0.9942	0.9964	+0.0022 -0.0022
2	Be + CH_2	0.9976	0.9996	1.0016	+0.0020 -0.0020

3	Be	0.9906	0.9930	0.9953	+0.0023 -0.0024
3	CH_2	0.9818	0.9838	0.9858	+0.0020 -0.0020
3	Be + CH_2	0.9961	0.9982	1.0004	+0.0022 -0.0021
4	Be	0.9891	0.9916	0.9942	+0.0026 -0.0025
5	Be	0.9858	0.9885	0.9912	+0.0027 -0.0027
5	CH_2	0.9869	0.9894	0.9919	+0.0025 -0.0025
6	Be	0.9832	0.9861	0.9890	+0.0029 -0.0029
7	Be	0.9881	0.9911	0.9942	+0.0031 -0.0030
7	CH_2	0.9984	1.0013	1.0043	+0.0030 -0.0029
Solution No. 3		*0.5698 g/ml*	*0.5672 g/ml*	*0.5646 g/ml*	—
1	Be	0.9972	0.9987	1.0003	+0.0016 -0.0015
2	Be	0.9939	0.9957	0.9974	+0.0017 -0.0018
3	Be	0.9986	1.0005	1.0024	+0.0019 -0.0019
3	Be + CH_2	0.9972	0.9990	1.0007	+0.0017 -0.0018
4	Be	0.9935	0.9956	0.9977	+0.0021 -0.0021
5	Be	0.9875	0.9897	0.9919	+0.0022 -0.0022
5	CH_2	0.9846	0.9866	0.9887	+0.0021 -0.0020
6	Be	1.0009	1.0033	1.0056	+0.0023 -0.0024
7	Be	0.9856	0.9881	0.9907	+0.0026 -0.0025
7	CH_2	1.0019	1.0044	1.0068	+0.0024 -0.0025

The uncertainty in fissile ^{233}U concentration is significant but does not exceed Δk_{eff} of ±0.0031 for any experiment.

2.1.2 Uncertainty in HF Content - The solution contained 0.3 wt-% hydrofluoric acid (HF) content. A sensitivity study was performed to consider changes of ±0.05 wt-% in HF content with the total solution density unchanged. The result of this change is to replace a small amount of HF with water or vice-versa. This only slightly alters the $H/^{233}U$ ratio with small changes also in the oxygen and fluorine content. The results of these calculations are given in Table 11.

Table 11. Effect on k_{eff} due to Uncertainty in the HF Content.

Solution No.	Sphere No.	Reflector	HF Content (wt-%)			Change (Δk_{eff})
			0.25	0.30	0.35	
1	1	Be	0.9957	0.9954	0.9951	+0.0003 -0.0003
1	2	Be	0.9937	0.9934	0.9931	+0.0003 -0.0003
1	3	Be	0.9952	0.9949	0.9946	+0.0003 -0.0003
1	3	Be + CH_2	1.0027	1.0024	1.0021	+0.0003 -0.0003
1	4	Be	0.9987	0.9984	0.9980	+0.0003 -0.0004
1	4	Be + CH_2	0.9961	0.9958	0.9954	+0.0003 -0.0003
1	5	Be	0.9960	0.9956	0.9952	+0.0004 -0.0004
1	5	CH_2	0.9909	0.9906	0.9902	+0.0003 -0.0003
1	5	Be + CH_2	0.9928	0.9925	0.9921	+0.0003 -0.0004
1	6	Be	0.9926	0.9922	0.9918	+0.0003 -0.0004
1	6	Be + CH_2	0.9931	0.9927	0.9923	+0.0004 -0.0004
2	1	Be	0.9911	0.9908	0.9906	+0.0003 -0.0002
2	2	Be	0.9945	0.9942	0.9939	+0.0003 -0.0003
2	2	Be + CH_2	0.9998	0.9996	0.9993	+0.0002 -0.0003
2	3	Be	0.9933	0.9930	0.9927	+0.0003 -0.0003
2	3	CH_2	0.9841	0.9838	0.9835	+0.0003 -0.0003
2	3	Be + CH_2	0.9985	0.9982	0.9980	+0.0003 -0.0002
2	4	Be	0.9919	0.9916	0.9913	+0.0003 -0.0003
2	5	Be	0.9888	0.9885	0.9882	+0.0003 -0.0003
2	5	CH_2	0.9897	0.9894	0.9891	+0.0003 -0.0003
2	6	Be	0.9865	0.9861	0.9857	+0.0004 -0.0004
2	7	Be	0.9915	0.9911	0.9907	+0.0004 -0.0004

2	7	CH_2	1.0017	1.0013	1.0010	+0.0004 -0.0003
3	1	Be	0.9990	0.9987	0.9985	+0.0003 -0.0003
3	2	Be	0.9959	0.9957	0.9954	+0.0002 -0.0003
3	3	Be	1.0007	1.0005	1.0002	+0.0002 -0.0003
3	3	Be + CH_2	0.9992	0.9990	0.9987	+0.0002 -0.0003
3	4	Be	0.9959	0.9956	0.9954	+0.0003 -0.0002
3	5	Be	0.9900	0.9897	0.9895	+0.0003 -0.0002
3	5	CH_2	0.9869	0.9866	0.9864	+0.0003 -0.0002
3	6	Be	1.0036	1.0033	1.0030	+0.0003 -0.0003
3	7	Be	0.9885	0.9881	0.9878	+0.0004 -0.0003
3	7	CH_2	1.0047	1.0044	1.0041	+0.0003 -0.0003

The uncertainty in HF content is insignificant but does not exceed Δk_{eff} of ± 0.0004 for any experiment.

2.1.3 Uncertainty in Solution Density - The solution densities are reported as 1.9712, 1.8386 and 1.6357 g/ml in Table 3. The number of significant digits provides some indication of the accuracy in this value. The sensitivity to total solution density was considered by altering these values by ±0.0005 g/ml. The densities of all solution components were simply scaled by the corresponding factor. The results of these calculations are compared to the benchmark-model specification in Table 12.

Table 12. Effect on k_{eff} due to Uncertainty in the Solution Density.

Sphere No.	Reflector	Solution Density (g/ml)			Change (Δk_{eff})
		Minimum	Nominal	Maximum	
Solution No. 1		*1.9707 g/ml*	*1.9712 g/ml*	*1.9717 g/ml*	—
1	Be	0.9952	0.9954	0.9955	+0.0001 -0.0002
2	Be	0.9933	0.9934	0.9936	+0.0002 -0.0001
3	Be	0.9947	0.9949	0.9951	+0.0002 -0.0002
3	Be + CH_2	1.0022	1.0024	1.0025	+0.0001 -0.0002
4	Be	0.9982	0.9984	0.9986	+0.0002 -0.0002
4	Be + CH_2	0.9956	0.9958	0.9959	+0.0001 -0.0002
5	Be	0.9954	0.9956	0.9958	+0.0002 -0.0002
5	CH_2	0.9904	0.9906	0.9908	+0.0002 -0.0002
5	Be + CH_2	0.9923	0.9925	0.9927	+0.0002 -0.0002
6	Be	0.9920	0.9922	0.9925	+0.0003 -0.0002
6	Be + CH_2	0.9925	0.9927	0.9929	+0.0002 -0.0002
Solution No. 2		*1.8381 g/ml*	*1.8386 g/ml*	*1.8391 g/ml*	—
1	Be	0.9907	0.9908	0.9910	+0.0002 -0.0001
2	Be	0.9940	0.9942	0.9944	+0.0002 -0.0002
2	Be + CH_2	0.9994	0.9996	0.9998	+0.0002 -0.0002
3	Be	0.9928	0.9930	0.9932	+0.0002 -0.0002
3	CH_2	0.9836	0.9838	0.9840	+0.0002 -0.0002
3	Be + CH_2	0.9981	0.9982	0.9984	+0.0002 -0.0001
4	Be	0.9914	0.9916	0.9918	+0.0002 -0.0002
5	Be	0.9883	0.9885	0.9887	+0.0002 -0.0002
5	CH_2	0.9892	0.9894	0.9896	+0.0002 -0.0002

6	Be	0.9859	0.9861	0.9863	+0.0002 -0.0002
7	Be	0.9909	0.9911	0.9914	+0.0003 -0.0002
7	CH_2	1.0011	1.0013	1.0016	+0.0003 -0.0002
Solution No. 3		*1.6352 g/ml*	*1.6357 g/ml*	*1.6362 g/ml*	—
1	Be	0.9985	0.9987	0.9989	+0.0002 -0.0002
2	Be	0.9955	0.9957	0.9959	+0.0002 -0.0002
3	Be	1.0003	1.0005	1.0007	+0.0002 -0.0002
3	Be + CH_2	0.9988	0.9990	0.9992	+0.0002 -0.0002
4	Be	0.9954	0.9956	0.9959	+0.0003 -0.0002
5	Be	0.9895	0.9897	0.9900	+0.0003 -0.0002
5	CH_2	0.9864	0.9866	0.9869	+0.0003 -0.0002
6	Be	1.0030	1.0033	1.0035	+0.0002 -0.0003
7	Be	0.9878	0.9881	0.9884	+0.0003 -0.0003
7	CH_2	1.0041	1.0044	1.0046	+0.0002 -0.0003

The uncertainty due to total solution density is insignificant and does not exceed Δk_{eff} of ±0.0003 for any experiment.

2.1.4 Uncertainty in Enrichment - The ^{233}U enrichment is specified as 98.562 percent by weight as given in Table 4. The number of significant digits in this value is an indication of accuracy. The sensitivity to enrichment or assay was considered by altering this value by ±0.005 wt-%. An increase in ^{233}U content was offset by a corresponding decrease in ^{238}U content and vice versa. The uncertainty in k_{eff} due to enrichment is negligible and does not exceed Δk_{eff} of ±0.00002 for any experiment which utilized Solution No. 1. Consequently, this uncertainty is assumed to also be negligible for the experiments with the other solutions.

2.2 Vessel Uncertainties

2.2.1 Uncertainty in Vessel Capacity - The capacities of the type 347 stainless steel vessels are given in Table 1 in grams of water. The benchmark specification assumes 1 gram of water is equivalent to 1 milliliter of volume as stated by the experimenter. However, it may be that the actual density of water used in performing these measurements was somewhat lower if the measurements were performed on a hot day. The sensitivity study considered this uncertainty by comparing the benchmark-model calculations to those where the capacity has been increased 0.5% by volume. This corresponds to a water density at temperatures in excess of 85 degrees F (or 30 degrees C). The vessel wall and reflector thicknesses are unchanged. The results of these calculations are given in Table 13 below.

Table 13. Effect on k_{eff} due to Vessel Capacity.

Solution No.	Sphere No.	Reflector	Vessel Capacity Increase		Change (Δk_{eff})
			0.5%	None	
1	1	Be	0.9968	0.9954	+0.0015
1	2	Be	0.9949	0.9934	+0.0015
1	3	Be	0.9964	0.9949	+0.0015
1	3	Be + CH_2	1.0037	1.0024	+0.0014
1	4	Be	0.9999	0.9984	+0.0015
1	4	Be + CH_2	0.9971	0.9958	+0.0014
1	5	Be	0.9971	0.9956	+0.0015
1	5	CH_2	0.9920	0.9906	+0.0014
1	5	Be + CH_2	0.9939	0.9925	+0.0015
1	6	Be	0.9938	0.9922	+0.0015
1	6	Be + CH_2	0.9942	0.9927	+0.0016
2	1	Be	0.9923	0.9908	+0.0015
2	2	Be	0.9957	0.9942	+0.0015
2	2	Be + CH_2	1.0009	0.9996	+0.0013
2	3	Be	0.9944	0.9930	+0.0014
2	3	CH_2	0.9851	0.9838	+0.0013
2	3	Be + CH_2	0.9996	0.9982	+0.0014
2	4	Be	0.9931	0.9916	+0.0015
2	5	Be	0.9900	0.9885	+0.0015
2	5	CH_2	0.9908	0.9894	+0.0014

2	6	Be	0.9877	0.9861	+0.0016
2	7	Be	0.9927	0.9911	+0.0016
2	7	CH_2	1.0029	1.0013	+0.0016
3	1	Be	1.0002	0.9987	+0.0015
3	2	Be	0.9972	0.9957	+0.0015
3	3	Be	1.0020	1.0005	+0.0015
3	3	Be + CH_2	1.0003	0.9990	+0.0013
3	4	Be	0.9971	0.9956	+0.0015
3	5	Be	0.9912	0.9897	+0.0015
3	5	CH_2	0.9881	0.9866	+0.0015
3	6	Be	1.0048	1.0033	+0.0015
3	7	Be	0.9897	0.9881	+0.0016
3	7	CH_2	1.0059	1.0044	+0.0015

The uncertainty due to vessel capacity is significant but does not exceed Δk_{eff} of –0.0000/+0.0016 for any experiment.

2.2.2 Uncertainty in Steel Composition - The elemental composition of type 347 stainless steel is given in Table 5. The sensitivity study investigated the uncertainty in composition of the actual vessels by comparing the nominal alloy specification (without impurities) to hypothetical compositions which minimize and maximize thermal neutron absorption as shown Table 14.

Table 14. Hypothetical Type 347 Stainless Steel Compositions.

Element	σ^a at 2200 m/s (barns)	Percent by Weight (wt-%)		
		Minimum [(a)]	Nominal	Maximum [(a)]
Fe	2.56	72.095	71.	65.
Cr	3.07	17.	18.	19.
Ni	4.49	9.	11.	13.
Mn	13.3			2.
Nb	1.15	1.		
Ta	20.6			1.
Si	0.171	0.75		
C	0.0035	0.08		
P	0.172	0.045		
S	0.52	0.030		

(a) In terms of neutron absorption.

The results of the k_{eff} calculations are recorded in Table 15.

Table 15. Effect on k_{eff} due to Uncertainty in the SS-347 Composition.

Solution No.	Sphere No.	Reflector	Neutron Absorption in SS-347			Change (Δk_{eff})
			Minimum	Nominal	Maximum	
1	1	Be	0.9954	0.9954	0.9945	+0.0000 -0.0009
1	2	Be	0.9935	0.9934	0.9928	+0.0001 -0.0006
1	3	Be	0.9949	0.9949	0.9945	+0.0004 -0.0000
1	3	Be + CH_2	1.0025	1.0024	1.0016	+0.0001 -0.0008
1	4	Be	0.9984	0.9984	0.9982	+0.0002 -0.0000
1	4	Be + CH_2	0.9958	0.9958	0.9952	+0.0000 -0.0006
1	5	Be	0.9956	0.9956	0.9955	+0.0000 -0.0001
1	5	CH_2	0.9906	0.9906	0.9901	+0.0000 -0.0004
1	5	Be + CH_2	0.9924	0.9925	0.9922	+0.0000 -0.0002

1	6	Be	0.9922	0.9922	0.9923	+0.0001 -0.0000
1	6	Be + CH_2	0.9927	0.9927	0.9926	+0.0000 -0.0001
2	1	Be	0.9909	0.9908	0.9899	+0.0001 -0.0009
2	2	Be	0.9942	0.9942	0.9936	+0.0000 -0.0006
2	2	Be + CH_2	0.9997	0.9996	0.9985	+0.0001 -0.0011
2	3	Be	0.9930	0.9930	0.9925	+0.0000 -0.0005
2	3	CH_2	0.9840	0.9838	0.9829	+0.0002 -0.0009
2	3	Be + CH_2	0.9984	0.9982	0.9974	+0.0002 -0.0008
2	4	Be	0.9916	0.9916	0.9914	+0.0000 -0.0002
2	5	Be	0.9885	0.9885	0.9884	+0.0000 -0.0001
2	5	CH_2	0.9894	0.9894	0.9889	+0.0000 -0.0005
2	6	Be	0.9861	0.9861	0.9862	+0.0001 -0.0000
2	7	Be	0.9911	0.9911	0.9913	+0.0002 -0.0000
2	7	CH_2	1.0013	1.0013	1.0013	+0.0000 -0.0000
3	1	Be	0.9988	0.9987	0.9976	+0.0001 -0.0011
3	2	Be	0.9957	0.9957	0.9949	+0.0000 -0.0008
3	3	Be	1.0005	1.0005	0.9999	+0.0000 -0.0006
3	3	Be + CH_2	0.9991	0.9990	0.9980	+0.0001 -0.0010
3	4	Be	0.9956	0.9956	0.9953	+0.0000 -0.0003
3	5	Be	0.9897	0.9897	0.9896	+0.0000 -0.0001
3	5	CH_2	0.9867	0.9866	0.9861	+0.0001 -0.0005
3	6	Be	1.0032	1.0033	1.0032	+0.0000 -0.0001
3	7	Be	0.9881	0.9881	0.9883	+0.0002 -0.0000
3	7	CH_2	1.0044	1.0044	1.0042	+0.0000 -0.0002

The uncertainty due to impurities present in type 347 stainless steel is insignificant and does not exceed Δk_{eff} of -0.0011/+0.0004 for any experiment.

2.2.3 **Uncertainty in Vessel Thickness** - The thicknesses of the type 347 stainless steel vessel walls were measured and reported as about 0.019 inches. The sensitivity study investigated uncertainties in the actual vessel wall thickness by assuming a 0.0005 inch (or half-a-mil) change which is consistent with the accuracy of the reported value. The resultant changes in k_{eff} are negligible and do not exceed Δk_{eff} of ± 0.0001 in any experiment which utilized Solution No. 1. Consequently, this uncertainty is assumed to also be negligible for the experiments with the other solutions.

2.2.4 **Uncertainty in Steel Density** - The nominal density of type 347 stainless steel is 8.0 g/cm^3 as reported in Section 1.3. The sensitivity study investigated uncertainties in the density by considering a ± 0.05 g/cm^3 change to the nominal value. The resultant changes in k_{eff} are negligible and do not exceed Δk_{eff} of ± 0.00003 for any experiment which utilized Solution No. 1. Consequently, this uncertainty is assumed to also be negligible for the experiments with the other solutions.

2.3 Reflector Uncertainties

2.3.1 **Uncertainty in the Critical Reflector Thickness** - Estimates of the experimental uncertainty in critical reflector thickness were recorded only for those experiments with reflection by beryllium metal as given in Table 2. The sensitivity study investigated this effect by calculating the k_{eff} for each system containing a beryllium metal reflector with the minimum and maximum thickness and comparing the result to the benchmark-model specification based on the nominal thickness. The resultant changes in k_{eff} are recorded in Table 16.

No estimates of the experimental uncertainty in critical reflector thickness have been found to date for the spheres with composite beryllium-polyethylene or polyethylene reflectors; consequently, a 3% uncertainty is assumed for these experiments. This uncertainty corresponds simply to the average uncertainty of the beryllium-reflected experiments rounded up to the nearest whole number.

Table 16. Effect on k_{eff} due to the Uncertainty in the Critical Reflector Thickness.

Solution No.	Sphere No	Reflector	Critical Reflector Thickness (cm)			Change (Δk_{eff})
			Minimum	Nominal	Maximum	
1	1	Be	0.9920	0.9954	0.9987	+0.0033 -0.0034
1	2	Be	0.9884	0.9934	0.9983	+0.0049 -0.0050
1	3	Be	0.9926	0.9949	0.9972	+0.0023 -0.0023
1	3	Be + CH_2	0.9981	1.0024	1.0063	+0.0039 -0.0043
1	4	Be	0.9923	0.9984	1.0044	+0.0060 -0.0061
1	4	Be + CH_2	0.9913	0.9958	1.0002	+0.0044 -0.0045
1	5	Be	0.9924	0.9956	0.9988	+0.0032 -0.0032
1	5	CH_2	0.9863	0.9906	0.9947	+0.0041 -0.0043
1	5	Be + CH_2	0.9873	0.9925	0.9975	+0.0050 -0.0052
1	6	Be	0.9893	0.9922	0.9952	+0.0030 -0.0029
1	6	Be + CH_2	0.9886	0.9927	0.9968	+0.0041 -0.0041
2	1	Be	0.9864	0.9908	0.9952	+0.0044 -0.0044
2	2	Be	0.9920	0.9942	0.9964	+0.0022 -0.0022
2	2	Be + CH_2	0.9974	0.9996	1.0016	+0.0020 -0.0022
2	3	Be	0.9887	0.9930	0.9972	+0.0042 -0.0043

2	3	CH_2	0.9837	0.9838	0.9839	+0.0001 -0.0001
2	3	Be + CH_2	0.9950	0.9982	1.0013	+0.0031 -0.0032
2	4	Be	0.9897	0.9916	0.9935	+0.0019 -0.0019
2	5	Be	0.9817	0.9885	0.9951	+0.0066 -0.0068
2	5	CH_2	0.9851	0.9894	0.9935	+0.0041 -0.0043
2	6	Be	0.9834	0.9861	0.9887	+0.0026 -0.0027
2	7	Be	0.9882	0.9911	0.9940	+0.0029 -0.0029
2	7	CH_2	0.9982	1.0013	1.0045	+0.0032 -0.0031
3	1	Be	0.9956	0.9987	1.0019	+0.0032 -0.0031
3	2	Be	0.9912	0.9957	1.0000	+0.0043 -0.0045
3	3	Be	0.9983	1.0005	1.0026	+0.0021 -0.0022
3	3	Be + CH_2	0.9960	0.9990	1.0017	+0.0027 -0.0030
3	4	Be	0.9927	0.9956	0.9985	+0.0029 -0.0029
3	5	Be	0.9811	0.9897	0.9981	+0.0084 -0.0086
3	5	CH_2	0.9824	0.9866	0.9907	+0.0041 -0.0042
3	6	Be	0.9974	1.0033	1.0090	+0.0057 -0.0059
3	7	Be	0.9842	0.9881	0.9920	+0.0039 -0.0039
3	7	CH_2	1.0011	1.0044	1.0076	+0.0032 -0.0033

The uncertainty due to the critical reflector thickness is significant but does not exceed Δk_{eff} of ±0.0086 for any experiment.

2.3.2 **Uncertainty in Reflector Density** - The average bulk density of the beryllium and polyethylene reflectors and the uncertainties in these values are reported in Table 6 and discussed in detail in Section 1.3. The sensitivity study investigated the effects of these uncertainties by calculating k_{eff} for each system using the minimum and maximum densities and comparing to the benchmark-model value based on the nominal density. The results are provided in Table 17.

Table 17. Effect on k_{eff} due to Uncertainty in Reflector Density.

Solution No.	Sphere No.	Reflector	Reflector Density			Change (Δk_{eff})
			Minimum	Nominal	Maximum	
1	1	Be	0.9879	0.9954	1.0003	+0.0049 -0.0075
1	2	Be	0.9869	0.9934	0.9978	+0.0044 -0.0065
1	3	Be	0.9891	0.9949	0.9988	+0.0039 -0.0058
1	3	Be + CH_2	0.9985	1.0024	1.0056	+0.0032 -0.0039
1	4	Be	0.9936	0.9984	1.0016	+0.0032 -0.0048
1	4	Be + CH_2	0.9926	0.9958	0.9986	+0.0028 -0.0032
1	5	Be	0.9917	0.9956	0.9983	+0.0027 -0.0039
1	5	CH_2	0.9882	0.9906	0.9929	+0.0023 -0.0024
1	5	Be + CH_2	0.9890	0.9925	0.9952	+0.0027 -0.0035
1	6	Be	0.9893	0.9922	0.9942	+0.0020 -0.0029
1	6	Be + CH_2	0.9903	0.9927	0.9948	+0.0021 -0.0024
2	1	Be	0.9834	0.9908	0.9957	+0.0049 -0.0074
2	2	Be	0.9877	0.9942	0.9986	+0.0044 -0.0065
2	2	Be + CH_2	0.9954	0.9996	1.0029	+0.0033 -0.0042
2	3	Be	0.9872	0.9930	0.9968	+0.0038 -0.0058
2	3	CH_2	0.9823	0.9838	0.9852	+0.0014 -0.0015
2	3	Be + CH_2	0.9943	0.9982	1.0015	+0.0033 -0.0039
2	4	Be	0.9869	0.9916	0.9948	+0.0032 -0.0047
2	5	Be	0.9846	0.9885	0.9911	+0.0026 -0.0039
2	5	CH_2	0.9870	0.9894	0.9917	+0.0023 -0.0024
2	6	Be	0.9832	0.9861	0.9880	+0.0019 -0.0029

2	7	Be	0.9891	0.9911	0.9924	+0.0013 -0.0020
2	7	CH_2	0.9999	1.0013	1.0028	+0.0015 -0.0014
3	1	Be	0.9913	0.9987	1.0037	+0.0050 -0.0074
3	2	Be	0.9891	0.9957	1.0001	+0.0044 -0.0066
3	3	Be	0.9946	1.0005	1.0044	+0.0039 -0.0059
3	3	Be + CH_2	0.9952	0.9990	1.0021	+0.0031 -0.0038
3	4	Be	0.9908	0.9956	0.9989	+0.0033 -0.0048
3	5	Be	0.9857	0.9897	0.9924	+0.0027 -0.0040
3	5	CH_2	0.9843	0.9866	0.9889	+0.0023 -0.0023
3	6	Be	1.0001	1.0033	1.0054	+0.0021 -0.0032
3	7	Be	0.9861	0.9881	0.9895	+0.0014 -0.0020
3	7	CH_2	1.0028	1.0044	1.0059	+0.0015 -0.0016

The uncertainty due to the range of reflector bulk density is significant but does not exceed Δk_{eff} of -0.0075/+0.0050 for any experiment.

2.3.3 **Uncertainty in Beryllium Composition** - There are no recorded impurities other than the maximum BeO content of 2 wt-%. However, typical commercially pure beryllium contains at least 98.0 wt-% beryllium (in all forms) together with the impurities as listed in Table 7.

The sensitivity study investigated the effect of these impurities by calculating the k_{eff} for each system containing beryllium metal with the maximum impurity content and comparing the result to the benchmark-model specification based on pure beryllium metal. The resultant changes in k_{eff} are recorded in Table 18.

Table 18. Effect on k_{eff} due to Impurities in Beryllium Metal.

Solution No.	Sphere No.	Reflector	Be Metal Impurities		Change (Δk_{eff})
			Maximum	None	
1	1	Be	0.9891	0.9954	-0.0063
1	2	Be	0.9881	0.9934	-0.0053
1	3	Be	0.9902	0.9949	-0.0047
1	3	Be + CH_2	1.0005	1.0024	-0.0019
1	4	Be	0.9945	0.9984	-0.0039

1	4	Be + CH_2	0.9949	0.9958	-0.0009
1	5	Be	0.9924	0.9956	-0.0032
1	5	CH_2	N/A	0.9906	-0.0000
1	5	Be + CH_2	0.9906	0.9925	-0.0019
1	6	Be	0.9899	0.9922	-0.0023
1	6	Be + CH_2	0.9917	0.9927	-0.0010
2	1	Be	0.9846	0.9908	-0.0062
2	2	Be	0.9888	0.9942	-0.0054
2	2	Be + CH_2	0.9968	0.9996	-0.0028
2	3	Be	0.9883	0.9930	-0.0047
2	3	CH_2	N/A	0.9838	-0.0000
2	3	Be + CH_2	0.9963	0.9982	-0.0019
2	4	Be	0.9878	0.9916	-0.0038
2	5	Be	0.9854	0.9885	-0.0031
2	5	CH_2	N/A	0.9894	-0.0000
2	6	Be	0.9838	0.9861	-0.0023
2	7	Be	0.9895	0.9911	-0.0016
2	7	CH_2	N/A	1.0013	-0.0000
3	1	Be	0.9923	0.9987	-0.0064
3	2	Be	0.9902	0.9957	-0.0055
3	3	Be	0.9956	1.0005	-0.0049
3	3	Be + CH_2	0.9970	0.9990	-0.0020
3	4	Be	0.9917	0.9956	-0.0039
3	5	Be	0.9865	0.9897	-0.0032
3	5	CH_2	N/A	0.9866	-0.0000
3	6	Be	1.0007	1.0033	-0.0026
3	7	Be	0.9866	0.9881	-0.0015
3	7	CH_2	N/A	1.0044	-0.0000

The uncertainty due to impurities in beryllium metal is significant but does not exceed Δk_{eff} of -0.0064/+0.0000 for any experiment.

2.4 Uncertainty Due to Room Return

The experiments are believed to have taken place within the shielded C-Vault of Building 110. This vault is in the shape of a large "D" with a central low density floor positioned above a ten foot deep pit. Figure 2 shows that the assembly mid-plane is at least three feet above the floor. Consequently, the closest concrete surface is at least thirteen feet distant from the center of the assembly. The shielding walls of the vault are five foot thick concrete; the roof is two foot thick concrete. A crude estimate of the sensitivity to room return was performed by reflecting the assembly with a spherical shell of air, thirteen feet in outer radius, followed by an effectively infinite thickness of concrete. The results are given in Table 19.

Table 19. Effect on k_{eff} due to Room Return.

Solution No.	Sphere No.	Reflector	Room Return		Change (Δk_{eff})
			Present	Absent	
1	1	Be	0.9958	0.9954	+0.0004
1	2	Be	0.9939	0.9934	+0.0005
1	3	Be	0.9955	0.9949	+0.0006
1	3	Be + CH_2	1.0033	1.0024	+0.0009
1	4	Be	0.9990	0.9984	+0.0006
1	4	Be + CH_2	0.9967	0.9958	+0.0009
1	5	Be	0.9963	0.9956	+0.0007
1	5	CH_2	0.9914	0.9906	+0.0008
1	5	Be + CH_2	0.9932	0.9925	+0.0007
1	6	Be	0.9930	0.9922	+0.0008
1	6	Be + CH_2	0.9934	0.9927	+0.0007
2	1	Be	0.9912	0.9908	+0.0004
2	2	Be	0.9947	0.9942	+0.0005
2	2	Be + CH_2	1.0002	0.9996	+0.0006
2	3	Be	0.9935	0.9930	+0.0005
2	3	CH_2	0.9838	0.9838	+0.0000
2	3	Be + CH_2	0.9991	0.9982	+0.0009
2	4	Be	0.9922	0.9916	+0.0006
2	5	Be	0.9892	0.9885	+0.0007
2	5	CH_2	0.9902	0.9894	+0.0008

2	6	Be	0.9869	0.9861	+0.0008
2	7	Be	0.9920	0.9911	+0.0009
2	7	CH_2	1.0021	1.0013	+0.0008
3	1	Be	0.9991	0.9987	+0.0004
3	2	Be	0.9961	0.9957	+0.0004
3	3	Be	1.0010	1.0005	+0.0005
3	3	Be + CH_2	0.9997	0.9990	+0.0007
3	4	Be	0.9963	0.9956	+0.0007
3	5	Be	0.9904	0.9897	+0.0007
3	5	CH_2	0.9874	0.9866	+0.0008
3	6	Be	1.0041	1.0033	+0.0008
3	7	Be	0.9890	0.9881	+0.0009
3	7	CH_2	1.0051	1.0044	+0.0007

The uncertainty due to room return is insignificant and does not exceed Δk_{eff} of -0.0000/+0.0009 for any experiment.

2.5 Total Uncertainty

The minimum (most negative) and maximum (most positive) uncertainty in k_{eff}, or Δk_{eff}, applicable to each individual *Falstaff* experiment, is provided in Table 20. These values are the statistical (root-mean-square) sum of the individual uncertainties reported in the previous sections for each experiment. The standard uncertainty in keff is estimated[a] as the square root of the product of the minimum and maximum uncertainties. The standard uncertainty in k_{eff} is estimated to be less than ±1% Δk_{eff} for all *Falstaff* experiments which is sufficiently small to qualify these experiments as acceptable benchmarks.

Table 20. Total Uncertainty for Each *Falstaff* Experiment

Experiment			Uncertainty in k_{eff} (or Δk_{eff})		
Solution No.	Sphere No.	Reflector	Minimum	Maximum	Standard
1	1	Be	-0.0106	+0.0064	±0.0083
1	2	Be	-0.0100	+0.0072	±0.0085
1	3	Be	-0.0082	+0.0054	±0.0066
1	3	Be + CH_2	-0.0066	+0.0058	±0.0061
1	4	Be	-0.0091	+0.0075	±0.0082
1	4	Be + CH_2	-0.0061	+0.0060	±0.0061
1	5	Be	-0.0066	+0.0053	±0.0059
1	5	CH_2	-0.0055	+0.0056	±0.0056
1	5	Be + CH_2	-0.0071	+0.0065	±0.0068
1	6	Be	-0.0055	+0.0050	±0.0053
1	6	Be + CH_2	-0.0056	+0.0057	±0.0057
2	1	Be	-0.0108	+0.0076	±0.0091
2	2	Be	-0.0090	+0.0056	±0.0071
2	2	Be + CH_2	-0.0060	+0.0046	±0.0052
2	3	Be	-0.0090	+0.0063	±0.0075
2	3	CH_2	-0.0027	+0.0028	±0.0028
2	3	Be + CH_2	-0.0058	+0.0053	±0.0055
2	4	Be	-0.0068	+0.0048	±0.0057
2	5	Be	-0.0089	+0.0078	±0.0083

[a] The American Mathematical Monthly, vol. 107, no. 4, pp. 353 – 357, April 2000, "A Better Bound on the Variance", Rajendra Bhatia and Chandler Davis.

2	5	CH_2	-0.0056	+0.0056	±0.0056
2	6	Be	-0.0054	+0.0047	±0.0050
2	7	Be	-0.0049	+0.0048	±0.0049
2	7	CH_2	-0.0045	+0.0050	±0.0047
3	1	Be	-0.0104	+0.0063	±0.0081
3	2	Be	-0.0099	+0.0066	±0.0081
3	3	Be	-0.0082	+0.0051	±0.0065
3	3	Be + CH_2	-0.0056	+0.0047	±0.0051
3	4	Be	-0.0072	+0.0052	±0.0061
3	5	Be	-0.0103	+0.0093	±0.0098
3	5	CH_2	-0.0052	+0.0054	±0.0053
3	6	Be	-0.0076	+0.0067	±0.0071
3	7	Be	-0.0053	+0.0052	±0.0053
3	7	CH_2	-0.0045	+0.0046	±0.0046

The uncertainties associated with the solution may contribute to systematic uncertainty in the calculated k_{eff} for each solution series which is estimated to be at most ±0.0032 Δk_{eff}. All other uncertainties are random.

3.0 BENCHMARK SPECIFICATIONS

3.1 Description of Model

The benchmark-model representation for each critical experiment is a one-dimensional spherical-geometry model consisting of three or four uniform regions corresponding to the solution, the steel vessel, and the reflector with a vacuum boundary condition applied to the outermost (reflector) surface of the sphere.

3.2 Dimensions

The model dimensions vary for each experiment depending on the vessel size and critical reflector thickness. The outer radii of each material region for each experiment are given in Table 21.

The vessel wall thickness was 0.019 inches (or 0.0483 cm) in all cases. The inner (solution) radius was based on the measured capacities given in Table 1 assuming one milliliter for each gram of water. The reflector radii were based on the reported critical thickness given in Table 2.

Table 21. Benchmark Model Outer Radial Dimensions in Centimeters.

Solution No.	Sphere No.	Solution	Steel	Beryllium	Polyethylene
1	1	7.8726	7.9209	15.9209	
1	2	8.5152	8.5635	14.3835	
1	3	9.0079	9.0562	13.7262	
1	3	9.0079	9.0562	10.1962	14.3062
1	4	9.6633	9.7116	13.2116	
1	4	9.6633	9.7116	10.2216	13.5316
1	5	10.1625	10.2107	12.9007	
1	5	10.1625	10.2107		13.2607
1	5	10.1625	10.2107	11.4807	12.9507
1	6	10.7992	10.8475	12.6775	
1	6	10.7992	10.8475	11.4875	12.8375
2	1	7.8726	7.9209	15.9209	
2	2	8.5152	8.5635	14.5035	
2	2	8.5152	8.5635	10.2135	15.3935
2	3	9.0079	9.0562	13.7562	
2	3	9.0079	9.0562		20.7362
2	3	9.0079	9.0562	10.1962	14.2562
2	4	9.6633	9.7116	13.1416	
2	5	10.1625	10.2107	12.8307	
2	5	10.1625	10.2107		13.2807
2	6	10.7992	10.8475	12.6275	
2	7	11.4152	11.4635	12.6435	
2	7	11.4152	11.4635		12.9835
3	1	7.8726	7.9209	16.6109	
3	2	8.5152	8.5635	14.7635	
3	3	9.0079	9.0562	14.0862	
3	3	9.0079	9.0562	10.1962	14.5362
3	4	9.6633	9.7116	13.3216	
3	5	10.1625	10.2107	12.9307	
3	5	10.1625	10.2107		13.3107
3	6	10.7992	10.8475	12.9275	
3	7	11.4152	11.4635	12.6535	
3	7	11.4152	11.4635		13.0635

3.3 Material Data

The solution models were based on the *best choice* from the reported data. The approach taken was to preserve all significant parameters within the reported experimental ranges; hence,

1. The fissile ^{233}U masses and concentrations are correct to the reported number of significant figures based on the benchmark-model concentrations of 0.866, 0.749 and 0.5672 $g^{233}U/cc$ as described in Section 2.1.1;

2. The uranium isotopics are as reported in Table 4 except that the ^{238}U content has been reduced to preserve the sum of the constituents as 100% of the whole.

3. The fissile concentrations and isotopics determine the UO_2F_2 concentrations in the models as 1.1425, 0.9882 and 0.7483 g/cm^3;

4. The solution densities are taken as the values reported by Kolar of 1.9712, 1.8386 and 1.6357 g/cm^3 in an internal LLNL memoranda which was reviewed by Ralston (without changes to these particular values);

5. The HF concentrations in the models are 0.0059, 0.0055 and 0.0049 g/cm^3 based on the reported HF content of 0.3 percent by weight of the solution; and,

6. The H_2O concentrations are then determined by difference as (1.9712 – 1.1425 – 0.0059) g/cm^3 = 0.8228 g/cm^3, (1.8386-0.9882-0.0055) g/cm^3 = 0.8449 g/cm^3, and (1.6357-0.7483-0.0049) g/cm^3 = 0.8825 g/cm^3.

The atom densities for each constituent of the solutions may now be calculated as provided in Table 22 below.

Table 22. Atom Densities for ^{233}U Solution.

Solution →	No. 1	No. 2	No. 3
Isotope or Nuclide	Atom Density (atoms/barn-cm)		
^{232}U	4.5608×10^{-8}	3.9445×10^{-8}	2.9871×10^{-8}
^{233}U	2.2379×10^{-3}	1.9355×10^{-3}	1.4657×10^{-3}
^{234}U	2.4316×10^{-5}	2.1030×10^{-5}	1.5925×10^{-5}
^{235}U	8.9598×10^{-7}	7.7491×10^{-7}	5.8682×10^{-7}
^{238}U	7.1284×10^{-6}	6.1652×10^{-6}	4.6687×10^{-6}
H	5.5183×10^{-2}	5.6654×10^{-2}	5.9146×10^{-2}
O	3.2043×10^{-2}	3.2171×10^{-2}	3.2474×10^{-2}
F	4.7182×10^{-3}	4.0930×10^{-3}	3.1214×10^{-3}

The atom densities given in Table 23 for the type 347 stainless steel vessel are based on the nominal alloy at 8.0 g/cm^3.

Table 23. Atom Densities for Type 347 Stainless Steel.

Nuclide	Composition (wt-%)	Atom Density (atoms/barn-cm)
Fe	71	6.1248×10^{-2}
Cr	18	1.6678×10^{-2}
Ni	11	9.0264×10^{-3}

The atom densities for the beryllium and polyethylene reflectors given in Table 24 are based on average bulk densities of 1.82 and 0.92 g/cm^3, respectively.

Table 24. Atom Densities for the Beryllium and Polyethylene Reflectors.

Material	Nuclide	Atom Density (atoms/barn-cm)
Beryllium	Be	1.2161×10^{-1}
Polyethylene (CH_2)	C	3.9497×10^{-2}
	H	7.8994×10^{-2}

3.4 Temperature Data

The temperature of the experiments is not known but is assumed to be ambient room temperature of about 20°C (70°F).

3.5 Experimental and Benchmark-Model k_{eff}

The experimental configurations are extrapolations to critical configurations. Therefore, the experimental k_{eff}'s are equal to one. Estimates of the uncertainty in k_{eff} due to the uncertainty in the various experimental parameters are provided in Section 2 with an estimate of the total uncertainty for each experiment given in Table 20. The experimental k_{eff} is then simply one plus-or-minus the standard uncertainty. These values are provided in Table 25.

Table 25. Experimental k_{eff}

Solution No.	Sphere No.	Reflector	Experimental k_{eff}
1	1	Be	1.0000 ± 0.0083
1	2	Be	1.0000 ± 0.0085
1	3	Be	1.0000 ± 0.0066
1	3	Be + CH_2	1.0000 ± 0.0061
1	4	Be	1.0000 ± 0.0082
1	4	Be + CH_2	1.0000 ± 0.0061
1	5	Be	1.0000 ± 0.0059
1	5	CH_2	1.0000 ± 0.0056
1	5	Be + CH_2	1.0000 ± 0.0068
1	6	Be	1.0000 ± 0.0053
1	6	Be + CH_2	1.0000 ± 0.0057
2	1	Be	1.0000 ± 0.0091
2	2	Be	1.0000 ± 0.0071
2	2	Be + CH_2	1.0000 ± 0.0052
2	3	Be	1.0000 ± 0.0075
2	3	CH_2	1.0000 ± 0.0028
2	3	Be + CH_2	1.0000 ± 0.0055
2	4	Be	1.0000 ± 0.0057
2	5	Be	1.0000 ± 0.0083
2	5	CH_2	1.0000 ± 0.0056
2	6	Be	1.0000 ± 0.0050
2	7	Be	1.0000 ± 0.0049
2	7	CH_2	1.0000 ± 0.0047
3	1	Be	1.0000 ± 0.0081
3	2	Be	1.0000 ± 0.0081
3	3	Be	1.0000 ± 0.0065

3	3	Be + CH_2	1.0000 ± 0.0051
3	4	Be	1.0000 ± 0.0061
3	5	Be	1.0000 ± 0.0098
3	5	CH_2	1.0000 ± 0.0053
3	6	Be	1.0000 ± 0.0071
3	7	Be	1.0000 ± 0.0053
3	7	CH_2	1.0000 ± 0.0046

4.0 RESULTS OF SAMPLE CALCULATIONS

Calculated k_{eff} results for a sample of United States codes are presented in Table 26. Calculated k_{eff} results for a sample code from France are provided in Table 27 courtesy of Jacques Anno of the Institut de Protection et de Surete Nucleaire (ISPN). Details of the SAN, KENO, VIM, MCNP, COG and APOLLO codes are provided in Appendix A. A typical input listing for each code is also provided in this appendix.

Table 26. Sample k_{eff} Calculational Results (United States).

Code → (Cross Section Set) →			SAN (92-Group L-DIV)	KENO (27-Group ENDF/B-IV)	VIM (Continuous Energy ENDF/B-V)	MCNP (Continuous Energy ENDF/B-VI)	COG (Continuous Energy ENDF-ENDL)
Sol'n No.	Sphere No.	Reflector					
1	1	Be	0.99537	1.0149 ± 0.0003	0.9969 ± 0.0002	0.9894 ± 0.0002	1.0067 ± 0.0003
1	2	Be	0.99343	1.0103 ± 0.0003	0.9924 ± 0.0002	0.9848 ± 0.0002	1.0042 ± 0.0003
1	3	Be	0.99492	1.0113 ± 0.0004	0.9929 ± 0.0002	0.9854 ± 0.0002	1.0057 ± 0.0003
1	3	Be+CH_2	1.00236	1.0167 ± 0.0003	0.9997 ± 0.0002	0.9953 ± 0.0002	1.0164 ± 0.0003
1	4	Be	0.99838	1.0137 ± 0.0003	0.9955 ± 0.0002	0.9885 ± 0.0002	1.0093 ± 0.0003
1	4	Be+CH_2	0.99577	1.0094 ± 0.0003	0.9910 ± 0.0002	0.9876 ± 0.0002	1.0107 ± 0.0003
1	5	Be	0.99562	1.0101 ± 0.0003	0.9920 ± 0.0006	0.9853 ± 0.0002	1.0074 ± 0.0003
1	5	CH_2	0.99057	1.0033 ± 0.0003	0.9846 ± 0.0006	0.9824 ± 0.0002	1.0064 ± 0.0003
1	5	Be+CH_2	0.99247	1.0049 ± 0.0003	0.9872 ± 0.0006	0.9819 ± 0.0002	1.0047 ± 0.0003
1	6	Be	0.99224	1.0052 ± 0.0003	0.9872 ± 0.0002	0.9820 ± 0.0002	1.0048 ± 0.0003
1	6	Be+CH_2	0.99272	1.0048 ± 0.0003	0.9865 ± 0.0002	0.9825 ± 0.0002	1.0059 ± 0.0003
1	Mean and Standard Deviation		0.9949 ±0.0033	1.0095 ± 0.0045	0.9910 ± 0.0047	0.9859 ± 0.0041	1.0075 ± 0.0036
2	1	Be	0.99083	1.0106 ± 0.0003	0.9932 ± 0.0002	0.9851 ± 0.0002	1.0028 ± 0.0003
2	2	Be	0.99422	1.0119 ± 0.0003	0.9936 ± 0.0002	0.9857 ± 0.0002	1.0047 ± 0.0003
2	2	Be+CH_2	0.99959	1.0146 ± 0.0003	0.9984 ± 0.0002	0.9932 ± 0.0002	1.0146 ± 0.0003
2	3	Be	0.99297	1.0088 ± 0.0003	0.9913 ± 0.0002	0.9838 ± 0.0002	1.0031 ± 0.0003
2	3	CH_2	0.98381	1.0023 ± 0.0003	0.9835 ± 0.0002	0.9813 ± 0.0002	1.0090 ± 0.0003
2	3	Be+CH_2	0.99824	1.0128 ± 0.0003	0.9956 ± 0.0002	0.9906 ± 0.0002	1.0118 ± 0.0003
2	4	Be	0.99161	1.0069 ± 0.0003	0.9888 ± 0.0002	0.9815 ± 0.0002	1.0032 ± 0.0003
2	5	Be	0.98851	1.0029 ± 0.0003	0.9845 ± 0.0002	0.9782 ± 0.0002	1.0009 ± 0.0003
2	5	CH_2	0.98938	1.0021 ± 0.0003	0.9833 ± 0.0002	0.9810 ± 0.0002	1.0051 ± 0.0003
2	6	Be	0.98611	0.9992 ± 0.0003	0.9813 ± 0.0002	0.9757 ± 0.0002	0.9992 ± 0.0003

2	7	Be	0.99111	1.0035 ± 0.0003	0.9857 ± 0.0002	0.9806 ± 0.0002	1.0043 ± 0.0003
2	7	CH_2	1.00134	1.0124 ± 0.0003	0.9943 ± 0.0002	0.9913 ± 0.0002	1.0165 ± 0.0003
2	Mean and Standard Deviation		0.9923 ±0.0053	1.0073 ± 0.0052	0.9895 ± 0.0057	0.9840 ± 0.0054	1.0063 ± 0.0055
3	1	Be	0.99874	1.0208 ± 0.0003	1.0029 ± 0.0002	0.9948 ± 0.0002	1.0124 ± 0.0003
3	2	Be	0.99567	1.0140 ± 0.0003	0.9959 ± 0.0002	0.9882 ± 0.0002	1.0067 ± 0.0003
3	3	Be	1.00047	1.0174 ± 0.0003	0.9995 ± 0.0002	0.9915 ± 0.0002	1.0116 ± 0.0003
3	3	Be+CH_2	0.99896	1.0130 ± 0.0003	0.9966 ± 0.0002	0.9918 ± 0.0002	1.0126 ± 0.0003
3	4	Be	0.99563	1.0109 ± 0.0003	0.9934 ± 0.0002	0.9858 ± 0.0002	1.0068 ± 0.0003
3	5	Be	0.98973	1.0039 ± 0.0003	0.9861 ± 0.0002	0.9794 ± 0.0002	1.0018 ± 0.0003
3	5	CH_2	0.98665	0.9994 ± 0.0003	0.9811 ± 0.0002	0.9782 ± 0.0002	1.0022 ± 0.0003
3	6	Be	1.00327	1.0170 ± 0.0003	0.9995 ± 0.0002	0.9928 ± 0.0002	1.0159 ± 0.0003
3	7	Be	0.98813	0.9997 ± 0.0003	0.9830 ± 0.0002	0.9773 ± 0.0002	1.0012 ± 0.0003
3	7	CH_2	1.00437	1.0151 ± 0.0003	0.9976 ± 0.0002	0.9940 ± 0.0002	1.0190 ± 0.0003
3	Mean and Standard Deviation		0.9962 ±0.0062	1.0111 ± 0.0076	0.9936 ± 0.0075	0.9874 ± 0.0068	1.0090 ± 0.0062

In several of the cross-section sets described in Table 25, cross-section data for ^{232}U is unavailable. In these cases the ^{234}U content has been increased to account for ^{232}U as stated in Appendix A.

Table 27. Sample k_{eff} Calculational Results (France).

Code → (Cross Section Set) →			APOLLO (20-Group CEA-93)	APOLLO (172-Group CEA-93)
Solution No.	Sphere No.	Reflector		
1	1	Be	1.0016	0.9973
1	2	Be	0.9949	0.9913
1	3	Be	0.9944	0.9916
1	3	Be + CH_2	1.0032	1.0009
1	4	Be	0.9961	0.9938
1	4	Be + CH_2	0.9936	0.9921
1	5	Be	0.9924	0.9903
1	5	CH_2	0.9869	0.9864
1	5	Be + CH_2	0.9886	0.9865
1	6	Be	0.9876	0.9860
1	6	Be + CH_2	0.9874	0.9859
1	Mean and Standard Deviation		0.9933 ± 0.0056	0.9911 ± 0.0049

5.0 REFERENCES

There are no published references.

APPENDIX A: TYPICAL CODE INPUT LISTINGS

A.1 Typical SAN Input Listing

An input listing for a SAN calculation using ultra-fine automatic meshing is provided below. SAN[a] is a short version of the ANISN code originally developed at ORNL and subsequently modified at LLNL. All SAN calculations were performed in the default $S_{12}P_3$ approximation and utilized a default, circa 1975, 92-group cross-section library developed by LLNL (L-Division) for criticality safety applications.

```
FALSTAFF; Sol'n No. 1; Sphere No. 1; 8.00 cm Be
sphere reflection vacuum
    1   u233       0   3   2.2379-3
    1   u234       0   3   2.4362-5
    1   u235       0   3   8.9598-7
    1   u238       0   3   7.1284-6
    1   h*h2o      0   3   5.5183-2
    1   o          0   3   3.2043-2
    1   f          0   3   4.7182-3
    2   fe         0   3   6.1248-2
    2   cr         0   3   1.6678-2
    2   ni         0   3   9.0264-3
    3   be*metal   0   3   1.2161-1
    last
  7.8726  0.1  1
  7.9209  0.1  2
 15.9209  0.1  3
last
end
```

Cross-section data for ^{232}U is not available in the 92-group LLNL cross-section library; consequently, the ^{234}U content has been increased to include ^{232}U and ^{234}U.

[a] Susan Post, *Summary Guide, Running SAN on UNIX Computers*, January 3, 2000.

A.2 Typical KENO Input Listing

An input deck for a KENO-Va[a] calculation using the CSAS25[b] module and the 27-group ENDF/B-IV SCALE cross-section library is provided below. The calculation used a total of 5050 generations, with 2500 neutrons per generation, and skipped 50 generations. This result is therefore based on 12.5 million active neutron histories.

```
=CSAS25
FALSTAFF; Sol'n No. 1; Sphere No. 1; 8.00 cm Be
27GROUPNDF4 INFHOMMEDIUM
U-233 1 0.0 2.2379-3 END
U-234 1 0.0 2.4362-5 END
U-235 1 0.0 8.9598-7 END
U-238 1 0.0 7.1284-6 END
H     1 0.0 5.5183-2 END
O     1 0.0 3.2043-2 END
F     1 0.0 4.7182-3 END
FE    2 0.0 6.1248-2 END
CR    2 0.0 1.6678-2 END
NI    2 0.0 9.0264-2 END
BE    3 0.0 1.2161-1 END
END COMP
READ PARAMETERS
  GEN=5050 NPG=2500 NSK=50 TME=2500
END PARAMETERS
READ GEOM
SPHERE 1 1  7.8726
SPHERE 2 1  7.9209
SPHERE 3 1 15.9209
END GEOMETRY
END DATA
END
```

Cross-section data for ^{232}U is not available in the 27-group ENDF/B-IV SCALE cross-section library; consequently, the ^{234}U content has been increased to include ^{232}U and ^{234}U.

---

[a] L. M. Petrie and N.F. Landers, *KENO V.a: An Improved Monte Carlo Criticality Program with Supergrouping*, NUREG/CR-0200, Revision 6, Volume 2, Section F11, ORNL/NUREG/CSD-2/R6, Oak Ridge National Laboratory, September 1998.

[b] N. F. Landers and L. M. Petrie, *CSAS: Control Module for Enhanced Criticality Safety Analysis Sequences*, NUREG/CR-0200, Revision 6, Volume 1, Section C4, ORNL/NUREG/CSD-2/V2/R6, Oak Ridge National Laboratory, September 1998.

A.3 Typical VIM Input Listing

An input deck for a VIM 3.6[a] calculation using a continuous ENDF/B-V cross-section library is provided below. The calculation used the maximum of 1000 generations, with 50000 neutrons per generation, and skipped 50 generations. This result is therefore based on 47.5 million active neutron histories.

```
1 FALSTAFF; Sol'n No. 1; Sphere No. 1; 8.00 cm Be              TYPE 01
  1000     3     0    50     0     0                                  TYPE 02
 50000 50000     1                                                   TYPE 03
     1     1     0     0    50     0                                  TYPE 04
    11     3     3     3     4 50000                                  TYPE 05
     9.0E+05     1.0E-05       275.0         1.0      1.0E-5  14.191E+06 TYPE 06AN
     9.5E-01     1.0E+01      1000.0         0.0                      TYPE 06BN
     1     0     0     0     3     0     0     0     0     0     0     0      07N
 30300 40300 603001003002103002203002303002603005703009003009303 00      TYPE 08
     0                                                               TYPE 09
     0                                                               TYPE 10
     0     0     5                                                   TYPE 20
  SPH    1        0.0       0.0       0.0    7.8726                  TYPE 21
  SPH    2        0.0       0.0       0.0    7.9209                  TYPE 21
  SPH    3        0.0       0.0       0.0   15.9209                  TYPE 21
  SPH    4        0.0       0.0       0.0   20.0000                  TYPE 21
  RPP    5       -8.0       8.0      -8.0       8.0      -8.0       8.0  TYPE 21
  END                                                                TYPE 21
  R01    6       1                                                   TYPE 22
  R02    6      -1       2                                          TYPE 22
  R03    6      -2       3                                          TYPE 22
  R04    6      -3       4                                          TYPE 22
  END                                                                TYPE 22
                                                                     TYPE 23
     1   101   1             2   200   2             3   300   3     TYPE 24
     4   000  -1                                                    TYPE 24
 30300 40300 60300100300260300570300900300                          TYPE 45
210300220300230300                                                  TYPE 45
930300                                                              TYPE 45
  8.9598E-07  7.1284E-06  2.4362E-05  2.2379E-03  3.2043E-02  4.7182E-03 TYPE 46
  5.5183E-02                                                        TYPE 46
  1.6678E-02  9.0264E-03  6.1248E-02                                TYPE 46
  1.2161E-01                                                        TYPE 46
  0.1000E+06  0.6250E+00  1.0000E-05                                TYPE 50
```

Cross-section data for ^{232}U is not available in the ENDF/B-V cross-section library; consequently, the ^{234}U content has been increased to include ^{232}U and ^{234}U.

[a] R. N. Blomquist, *VIM 3.6, Continuous Energy Neutron and Photon Transport Code System*, CCC-658, Oak Ridge National Laboratory, Radiation Shielding Information Computational Center, December 1998.

A.4 Typical MCNP Input Listing

The input listing for an MCNP4C[a] calculation using continuous-energy ENDF/B-VI, Release 2, cross sections is provided below. The calculation employed a total of 5200 generations and 5000 neutrons per generation. The first 200 generations were skipped so that the result is based on 25.0 million active neutron histories.

```
FALSTAFF; Sol'n No. 1; Sphere No. 1; 8.00 cm Be
     1 1 -1.9712 -1
     2 2 -8.00    1 -2
     3 3 -1.82    2 -3
     4 0          3

     1 so  7.8726
     2 so  7.9209
     3 so 15.9209

imp:n 1 1 1 0
    m1 92232.60c 4.5608-8 92233.60c 2.2379-3 92234.60c 2.4316-5 &
       92235.60c 8.9598-7 92238.60c 7.1284-6  1001.60c 5.5183-2 &
        8016.60c 3.2043-2  9019.60c 4.7182-3
   mt1  lwtr.01t
    m2 26054.60c 0.3552-2 26056.60c 5.6226-2 26057.60c 0.1286-2 &
       26058.60c 0.0184-2 24050.60c 0.0726-2 24052.60c 1.3974-2 &
       24053.60c 0.1584-2 24054.60c 0.0394-2 28058.60c 6.1623-3 &
       28060.60c 2.3560-3 28061.60c 0.1020-3 28062.60c 0.3240-3 &
       28064.60c 0.0821-3
    m3  4009.60c 1.
   mt3    be.01t
kcode 5000 1. 200 5200
  ksrc 0. 0. 0.
```

[a] Judith F. Briesmeister, Ed., *MCNP™ – A General Monte Carlo N-Particle Transport Code, Version 4C*, LA-13709-M, Los Alamos National Laboratory, April 10, 2000.

A.5 Typical COG Input Listing

The input listing for a COG[a] calculation using continuous ENDF-ENDL cross sections is provided below. This library contains low energy ENDF/B-VI data (for energies below about 20 keV) and high energy ENDL data. The calculation employed a total of 5020 generations and 5000 neutrons per generation. The first 20 generations were skipped so that the result is based on 25.0 million active neutron histories.

```
Sol'n No. 1; Sphere No. 1; 1.77 kg U-233 @ H/U=24.3; 8.00 cm Be
basic
   neutron delayedn CENTIMETERS
criticality
   npart=5000 nbatch=5020 sdt=0.0001 nfirst=21 norm=1.
   nsource=1  0. 0. 0.
mix nlib=ENDFB6
   mat=1  u233 0.86602  u234 0.00947  u235 0.00035  u238 0.00282
             o 0.12064     f 0.14325
        h(h2o) 0.00030     f 0.00560
        h(h2o) 0.09207     o 0.73068
   mat=2    fe 5.68       cr 1.44       ni 0.88
   mat=3    be 1.82
geometry
   sector 1 Soln   -1
   sector 2 SS347   1 -2
   sector 3 Be      2 -3
   boundary vacuum     3
picture cs material
  -16   0  16     -16   0 -16      16   0 -16
volume material
  -16 -16 -16      16 -16 -16     -16  16 -16
   32 32 32
surfaces
   1 sphere  7.8726
   2 sphere  7.9209
   3 sphere 15.9209
end
```

Cross-section data for ^{232}U is not available in the ENDF-ENDL cross-section library; consequently, the ^{234}U content has been increased to include ^{232}U and ^{234}U.

---

[a] Richard Buck, DeLynn Clark, Stella Hadjimarkos and Edward Lent, *COG: A Monte Carlo Neutron, Photon and Electron Transport Code; User's Manual, Second Edition*, Lawrence Livermore National Laboratory, July 4, 1994.

A.6 Typical APOLLO Input Listing

The input listing for an APOLLO calculation is given below as provided by of Jacques Anno of the Institut de Protection et de Surete Nucleaire (ISPN). APOLLO is an S_n transport calculation in the S_8P_3 approximation using a 20-group cross-section library which is collapsed from the 172-group, release V4, CEA-93 library, derived from JEFF.

```
DEBUT_APOLLO2
*=+=+=+=+=+=+=+=+=+=+=+=+=+=+=+=+=+=+=+=+=+=+=+=+=+=+=+=+=+=+=+=+
*      CIGALES version 1.0   en date du 06/01/2000
*                Creation du Fichier le 24/07/00 14:58:59
*=+=+=+=+=+=+=+=+=+=+=+=+=+=+=+=+=+=+=+=+=+=+=+=+=+=+=+=+=+=+=+=+
*                    -=- INITIALISATION - CALCUL 1 -=-
CALCUL_CRISTAL = 1                                                  ;
REPPROC             = OUVRIR: 22 'VARIABLE' 1024 10000
                               'ADRESSE' 'aprocristal'               ;
CHARGE_APROCRISTAL = LIRE: REPPROC 'APROC' 'CHARGE_APROCRISTAL'      ;
FERMER: REPPROC                                                     ;
EXECUTER CHARGE_APROCRISTAL                                         ;
TSTR TOPT = INITIALISER_CRISTAL 1                                   ;
*             -=- OPTIONS -=-
*
TOPT.'STCRI'.'NGROUP_FINAL' = 20                                    ;
TOPT.'STCRI'.'ANISOTROPIE'  = 'P3'                                  ;
*
*===============================================================
* APOLLO SN KEFF CALCUL  1
*===============================================================
*
TITRE: 'SN KEFF 1D                                  B= 1 V=7.8726' ;
*SN KEFF 1D                                    B= 1 V=7.8726 CAS 1

WRITE: TOPT.'RESU' 'SN1D '
'B= 1 V=7.8726 CAS 1'                                                ;
*
*             -=- Description des milieux -=-
* Milieu UO2F2
WRITE: TOPT.'RESU' ' Milieu UO2F2          '                          ;
nom_calc =  'MILHOM1'                                               ;
TOPT.'STCRI'.'CALCUL_INITIAL' = nom_calc                            ;
TOPT.'STCRI'.'CALCULS_INITIAUX'.nom_calc = TABLE:                   ;
TSTR.nom_calc = TABLE:                                              ;
*
nom_mil = 'Milieu UO2F2'                                            ;
TOPT.'STMIL'.nom_mil = TABLE:                                       ;
TOPT.'STMIL'.nom_mil.'U232     '  =    4.56000E-08                  ;
TOPT.'STMIL'.nom_mil.'U233     '  =    2.23790E-03                  ;
TOPT.'STMIL'.nom_mil.'U234     '  =    2.43160E-05                  ;
TOPT.'STMIL'.nom_mil.'U235     '  =    8.95900E-07                  ;
TOPT.'STMIL'.nom_mil.'U238     '  =    7.12840E-06                  ;
TOPT.'STMIL'.nom_mil.'H2O      '  =    2.75915E-02                  ;
TOPT.'STMIL'.nom_mil.'O16      '  =    4.45150E-03                  ;
TOPT.'STMIL'.nom_mil.'F19      '  =    4.71820E-03                  ;
TOPT.'STMIL'.nom_mil.'TEMPERATURE'  =  21.                          ;
*
TRES TSTR TOPT = GENERE_MILIEUX_S 2 TSTR TOPT                       ;
```

```
*
*                          -=- Creation de la geometrie -=-
*
TSTR.nom_calc.'GEO' = GEOM: &CYLI &MAIL 1 &EQD 1.
                            &MILI TSTR.'MILREF'.nom_mil  1          ;
*
*            -=- Creation de la bibliotheque interne -=-
*
TSTR.'APOLIB' = BIBINT: &EDIT 1 TSTR.'IDB' TSTR.nom_calc.'GEO'
                                ( TEXTE TOPT.'REPBIB' )             ;
*
*            -=-  autoprotection -=-
*
TSTR.'GEOAU' = TSTR.nom_calc.'GEO'                                  ;
*
TRES TSTR TOPT = AUTOPROTECTION_CRI_S 1 TSTR TOPT                   ;
*
*            -=- Flux a B2 nul -=-
*
TOPT.'TYPE_B2' = 'NUL'                                              ;
TRES TSTR TOPT = CALFLUX_PIJ_CRI_S 1 TSTR TOPT                      ;
*
*            -=- Flux a B2 critique -=-
*
SI ( TRES.'KINF' GT 1. )                                            ;
TOPT.'TYPE_B2' = 'CRITIQUE'                                         ;
TRES TSTR TOPT = CALFLUX_PIJ_CRI_S 1 TSTR TOPT                      ;
FINSI                                                               ;
*
TOPT.'STCRI'.'CALCULS_INITIAUX'.nom_calc.'B2' = TRES.'B2'           ;
TOPT.'STCRI'.'CALCULS_INITIAUX'.nom_calc.'KINF' = TRES.'KINF'       ;
*
*            -=- Condensation homogeneisation  -=-
*
TRES TSTR TOPT = HOMOGE_COND_S  1 TSTR TOPT                         ;
************************************************************
*    >>>>> REFLECTEUR  1
*
*ACIER

WRITE: TOPT.'RESU' 'ACIER                    '                        ;
TSTR TOPT = INITIALISER_CRISTAL 1 TSTR TOPT                         ;
*
nom_calc =  'REFLEC1'                                               ;
TOPT.'STCRI'.'CALCUL_INITIAL' = nom_calc                            ;
TOPT.'STCRI'.'CALCULS_INITIAUX'.nom_calc = TABLE:                   ;
TSTR.nom_calc = TABLE:                                              ;
*
nom_mil = 'ACIER'                                                   ;
TOPT.'STMIL'.nom_mil = TABLE:                                       ;
TOPT.'STMIL'.nom_mil.'U235'     =    1.E-10                         ;
TOPT.'STMIL'.nom_mil.'FENAT '  =       6.1248E-02                  ;
TOPT.'STMIL'.nom_mil.'CRNAT '  =       1.6678E-02                  ;
TOPT.'STMIL'.nom_mil.'NINAT '  =       9.0264E-03                  ;
TOPT.'STMIL'.nom_mil.'TEMPERATURE'  =  21.                          ;
*
TRES TSTR TOPT = GENERE_MILIEUX_S 2 TSTR TOPT                       ;
*
*                        -=- Creation de la geometrie  -=-
*
```

```
TSTR.nom_calc.'GEO' = GEOM: &CYLI &MAIL 1 &EQD 1.
                            &MILI TSTR.'MILREF'.nom_mil  1          ;
*
*            -=- Creation de la bibliotheque interne -=-
*
TSTR.'APOLIB' = BIBINT: &EDIT 1 TSTR.'APOLIB'
                                TSTR.'IDB' TSTR.nom_calc.'GEO'
                                ( TEXTE TOPT.'REPBIB' )            ;
*
*            -=- Flux a B2 nul -=-
*
TOPT.'TYPE_B2' = 'NUL'                                             ;
TRES TSTR TOPT = CALFLUX_PIJ_CRI_S 1 TSTR TOPT                     ;
TOPT.'STCRI'.'CALCULS_INITIAUX'.nom_calc.'B2' = TRES.'B2'          ;
*
*            -=- Condensation homogeneisation  -=-
*
TRES TSTR TOPT = HOMOGE_COND_S  1 TSTR TOPT                        ;
************************************************************
*    >>>>> REFLECTEUR  2
*
* Milieu Autre

WRITE: TOPT.'RESU' ' Milieu Autre          '                         ;
TSTR TOPT = INITIALISER_CRISTAL 1 TSTR TOPT                        ;
*
nom_calc =  'REFLEC2'                                              ;
TOPT.'STCRI'.'CALCUL_INITIAL' = nom_calc                           ;
TOPT.'STCRI'.'CALCULS_INITIAUX'.nom_calc = TABLE:                  ;
TSTR.nom_calc = TABLE:                                             ;
*
nom_mil = 'Milieu Autre'                                           ;
TOPT.'STMIL'.nom_mil = TABLE:                                      ;
TOPT.'STMIL'.nom_mil.'U235'     =    1.E-10                        ;
TOPT.'STMIL'.nom_mil.'BE9 '  =         1.21610E-01                ;
TOPT.'STMIL'.nom_mil.'TEMPERATURE'  =  21.                         ;
*
TRES TSTR TOPT = GENERE_MILIEUX_S 2 TSTR TOPT                      ;
*
*                       -=- Creation de la geometrie  -=-
*
TSTR.nom_calc.'GEO' = GEOM: &CYLI &MAIL 1 &EQD 1.
                            &MILI TSTR.'MILREF'.nom_mil  1         ;
*
*            -=- Creation de la bibliotheque interne -=-
*
TSTR.'APOLIB' = BIBINT: &EDIT 1 TSTR.'APOLIB'
                                TSTR.'IDB' TSTR.nom_calc.'GEO'
                                ( TEXTE TOPT.'REPBIB' )            ;
*
*            -=- Flux a B2 nul -=-
*
TOPT.'TYPE_B2' = 'NUL'                                             ;
TRES TSTR TOPT = CALFLUX_PIJ_CRI_S 1 TSTR TOPT                     ;
TOPT.'STCRI'.'CALCULS_INITIAUX'.nom_calc.'B2' = TRES.'B2'          ;
*
*            -=- Condensation homogeneisation  -=-
*
TRES TSTR TOPT = HOMOGE_COND_S  1 TSTR TOPT                        ;
*
```

```
*            -=- CREATION DE LA MACROLIB -=-
*                                -=- Options -=-
TOPT.'STCRI'.'B2'  = 0.                                                    ;
*                                -=- Calcul -=-
TRES TSTR TOPT = MACRO_GLOBALE_S 1 TSTR TOPT                               ;
*
*          <<<< CALCUL FINAL >>>>
*
*            -=- Géométrie -=-
TSTR.'GEO_SN' = GEOM:  &SPHE &MAIL &X
 10 &EQD 7.8726
 1 &EQD 7.9209
 7 &EQD 15.9209
 &MILI
       TSTR.'MILHOM1'.'MILEQ'  1  &A  10
       TSTR.'REFLEC1'.'MILEQ'  11
       TSTR.'REFLEC2'.'MILEQ'  12  &A  18
                                                                           ;
*
*            -=- Options -=-
TOPT.'STCRI'.'DIM'            = 1                                          ;
TOPT.'STCRI'.'TXT_CDL'        = '&VIDE'                                    ;
TOPT.'STCRI'.'TYPGEO'         = 'SPHERIQUE'                                ;
TOPT.'STCRI'.'ACCELERATION'   = 'SIM'                                      ;
TOPT.'STCRI'.'PRECI'          = 1.E-5                                      ;
TOPT.'STCRI'.'QUADRATURE'     = 8                                          ;
TOPT.'STCRI'.'NBEXT'          = 150                                        ;
*
*            -=- Flux -=-
TRES TSTR TOPT = CALCUL_SN_S 2 TSTR TOPT                                   ;
*
FERMER: ( TEXTE TOPT.'REPBIB' )                                            ;
DETRUIRE: TSTR TOPT TRES  nom_calc nom_mil                                 ;
*
EDTIME: ;
ARRET: ;
FIN_APOLLO2
*=*=*=*=*=*=*=*=*=*=*=*=*=*=*=*=*=*=*=*=*=*=*=*=*=*=*=*=*=*=*=*=*=*=*=*=*
*      CIGALES version 1.0   en date du 06/01/2000
*=*=*=*=*=*=*=*=*=*=*=*=*=*=*=*=*=*=*=*=*=*=*=*=*=*=*=*=*=*=*=*=*=*=*=*=*
*                   RAPPEL GEOMETRIE   SN KEFF 1D
*_____________________________________________________________________
* GEOMETRIE SPHERIQUE   BIBLIO CEA93.V4 ANISOTROPIE P3 ORDRE SN 8
*_____________________________________________________________________
* ZONES    1       2       3
* NB PTS  1       1       1
* EPAIS    B       0.0483  8.0
* CHIMIE   AUTRE   ACIER   AUTRE
*=====================================================================
(
SN KEFF 1D                                          B= 1 V=7.8726 CAS 1
SN1D  $B= 1 V=7.8726 CAS 1
)
OPTION V4 GROUP 20 P3 ORDRE 8 FINOPTION
SNKEFF   SPHERE
 3        10 7.8726
          1 7.9209
          7 15.9209
* Milieu UO2F2
GEOMETRIE HOMOGENE
```

U233-SOL-INTER-001

```
CHIMIE
* Milieu UO2F2
 MICRO 1 8
    U232 U233 U234 U235 U238 H2O O16 F19
   CONC   4.56E-08  .0022379  2.4316E-05  8.959E-07  7.1284E-06
   .0275915  .0044515  .0047182
FINC
*ACIER
GEOMETRIE HOMOGENE
CHIMIE
*ACIER
   MICRO 1 3 FENAT CRNAT NINAT CONC 0.061248 0.016678 0.0090264
FINC
* Milieu Autre
GEOMETRIE HOMOGENE
CHIMIE
* Milieu Autre
 MICRO 1 1
    BE9
   CONC   .12161
FINC
FIND
```

APPENDIX B: FISSION SPECTRA

COG calculated results for the median energy of those neutrons which produce fission events (i.e., the median fission energy) together with the fraction of fissions produced by neutrons in the thermal, intermediate and fast energy ranges are presented in Table 28. Note that the calculated intermediate fission fraction exceeds 50% for all experiments; hence, these experiments are said to have intermediate spectra.

Table 28. COG Calculated Fission Spectra.

Experiment			Median Fission Energy (eV)	Fission, %		
Solution No.	Sphere No.	Reflector		Thermal (< 0.625 eV)	Intermediate (0.625 eV – 100 keV)	Fast (> 100 keV)
Intermediate Fission Spectra						
1	5	Be	3.585	30.90	61.76	7.34
1	6	Be	3.730	30.68	61.76	7.56
1	4	Be	3.454	31.19	61.66	7.15
1	3	Be	3.249	31.72	61.37	6.91
1	2	Be	2.978	32.36	60.95	6.69
1	1	Be	2.309	33.90	59.78	6.32
1	6	Be + CH_2	2.528	33.95	58.79	7.26
1	5	Be + CH_2	2.366	34.39	58.50	7.11
2	6	Be	2.053	35.30	58.18	6.52
2	7	Be	2.069	35.22	58.14	6.64
2	5	Be	2.008	35.56	58.12	6.32
2	4	Be	1.982	35.82	58.02	6.16
2	3	Be	1.937	36.39	57.68	5.93
2	2	Be	1.889	37.03	57.24	5.73
2	1	Be	1.786	38.43	56.12	5.45
2	7	CH_2	1.757	39.16	54.64	6.20
1	5	CH_2	1.689	40.80	52.63	6.57
1	4	Be + CH_2	1.651	41.40	52.15	6.45
1	3	Be + CH_2	1.530	42.92	50.85	6.23
3	7	Be	1.294	44.30	50.73	4.97
3	6	Be	1.269	44.51	50.69	4.80
3	5	Be	1.258	44.60	50.67	4.73
3	4	Be	1.224	44.88	50.52	4.60

3	3	Be	1.156	45.45	50.16	4.39
Mixed Fission Spectra						
3	2	Be	1.087	46.01	49.71	4.28
2	5	CH_2	1.266	44.91	49.45	5.64
3	1	Be	0.900	47.50	48.47	4.03
2	3	Be + CH_2	1.054	46.69	47.92	5.39
3	7	CH_2	0.831	48.10	47.30	4.60
2	2	Be + CH_2	0.890	47.86	46.90	5.24
Thermal Fission Spectra						
3	5	CH_2	0.420	52.78	42.99	4.23
3	3	Be + CH_2	0.328	54.43	41.54	4.03
2	3	CH_2	0.447	52.12	42.88	5.00